STIC-ILL

From: Schnizer, Richard
Sent: Tuesday, June 15, 2004 1:13 PM
To: STIC-ILL
Subject: 09/555,574

Please send me a copy of :

Radley et al (Molecular Crystals and Liquid Crystals Science and Technology, Section A: Molecular Crystals nad Liquid Crystals (1997), 303: 249-254

Ziady et al (Am. J. Physiol. (197) 273(2, part 1): G545-G552)

Legendre et al (Bioconj. Chem. (1997) 8(1): 57-63)

Washwa et al (Bioconjugate Chemistry (1997) 8(1): 81-88

Thank you-

Richard Schnizer, Ph.D.
Patent Examiner
Art Unit 1635
Remsen 2C01
571-272-0762
Mail Box 2C18

Dioleoylmelittin as a Novel Serum-Insensitive Reagent for Efficient Transfection of Mammalian Cells

J. Y. Legendre,* A. Trzeciak, B. Bohrmann, U. Deuschle, E. Kitas, and A. Supersaxo

Preclinical Research and Development, F. Hoffmann-La Roche AG, CH-4070 Basel, Switzerland.
Received August 29, 1996®

Amphipathic peptides can be useful effectors to enhance gene delivery. However, peptide/DNA complexes usually require additional effectors, such as fusogenic lipids, to mediate efficient transfection. Due to weak and/or multiple interactions between the various components of the system, the transfecting complexes are often heterogeneous and unstable in biological fluids. Accordingly, a hybrid molecule resulting from the covalent coupling of an amphipathic, membrane-disturbing peptide to a lipid moiety might create a stable and efficient peptide-based gene transfer system. The present work describes such a novel hybrid molecule, dioleoylmelittin, resulting from the conjugation of dioleoylphosphatidylethanolamine-*N*-[3-(2-pyridyldithio)propionate] with [Cys^1]melittin. Dioleoylmelittin had a lower hemolytic and membrane-disturbing activity than melittin. Size and zeta potential measurements, DNA gel electrophoresis, and electron microscopy showed that dioleoylmelittin, unlike melittin, was able to complex plasmid DNA to form spherical particles with a net positive charge and a diameter between 50 and 250 nm. These particles, prepared at an optimal 10/1 dioleoylmelittin/DNA ratio (w/w), mediated efficient transient transfection of reporter genes in cultured mammalian cells including primary cells. The luciferase activity induced by the dioleoylmelittin/DNA complex was 5−500-fold higher than that induced by a cationic lipid/DNA complex, depending on the cationic lipid and the cell-line. Surprisingly, the presence of 10−50% fetal calf serum during dioleoylmelittin-mediated transfection enhanced 1.5−3-fold gene expression. Dioleoylmelittin represents a new class of efficient peptide-based transfection reagents, especially suited for serum-sensitive cells.

INTRODUCTION

Gene delivery is recognized as a key issue in the future development of gene therapy. Indeed, several recent gene therapy clinical trials in humans have shown the limitations of viruses to deliver genes (*1*). Nonviral gene delivery systems could therefore provide an easier and safer alternative to viruses (*2*). However, the transfection efficiency of synthetic carriers is still lower than that of viral vectors.

Cationic lipids are the most widely used nonviral transfection reagents both in cell culture and in animals (*3*, *4*). These transfection competent molecules are composed of a cationic moiety, which binds DNA by charge interactions, and a lipophilic tail. Therefore, cationic lipids have the dual ability of condensing DNA and fusing or destabilizing cell membranes (*3*, *4*). Another emerging gene transfer strategy is the use of amphipathic peptides (*5*−*11*). These peptides are either fusogenic or permeabilize cell membranes and, hence, improve gene transfer. For example, the cyclic peptide gramicidin S can facilitate DNA delivery into cells in culture (*8*−*10*). However, efficient transfection with this peptide requires the addition of co-lipids such as dioleoylphosphatidylethanolamine (DOPE) or short-chain phospholipids; both interact with the hydrophobic face of the gramicidin S (*8*, *9*). This binding usually occurs via weak interactions, and as a result, the transfecting particles are rather heterogeneous and unstable in biological fluids. Accordingly, hybrid molecules resulting from the covalent binding of a lipid moiety onto an amphipathic peptide might provide single, stable transfection competent reagents. The present work describes the synthesis of such a novel hybrid molecule, dioleoylmelittin. Melittin, a 26 amino acid peptide, is a well-characterized membrane-disturbing molecule (*12*). When complexed with plasmid DNA, its lipophilic derivative, dioleoylmelittin, forms homogeneous and small particles that mediate highly efficient transfection of cells in culture, even in the presence of serum.

MATERIALS AND METHODS

Synthesis of the Dioleoylmelittin. Continuous-flow solid-phase peptide synthesis was performed on a Milligen 9050 synthesizer, starting from a Tenta Gel S resin (0.22 mmol/g, Rapp Polymere, Tübingen, Germany), as described (*13*). All chiral amino acids were of the L-configuration. The base-labile 9-fluorenylmethyloxycarbonyl (Fmoc) group was used for α-amino protection. Side chains were protected with the following protecting groups: 2,2,5,7,8-pentamethylchroman-6-sulfonyl (Pmc) for arginine, triphenylmethane (Trt) for cysteine and glutamine, *tert*-butoxycarbonyl (Boc) for lysine and tryptophan, and *tert*-butyl (But) for serine and threonine. Fmoc-amino acids (2.5 equival) were activated with an equivalent amount of 1,1,3,3-tetramethyl-2-(2-oxo)-1(2*H*)-pyridyluronium tetrafluoroborate (*14*) and diisopropylethylamine. Fmoc deprotection was achieved with 20% (v/v) piperidine in dimethylformamide. The resin-bound peptide was treated with a mixture of 86% trifluoroacetic acid, 10% ethanedithiol, and 4% water for 3 h. The reaction mixture was concentrated and poured into diethyl ether, and the precipitate was collected by filtration and lyophilized from water. The crude peptide was purified by preparative HPLC. The fractions of the main peak were collected, concentrated under reduced pressure, and lyophilized, yielding 94.5 mg of compound **I** (CIGAVLKVLTTGLPALISWIKRKRQQ). The homogeneity of compound **I** was confirmed by analytical reversed

* Address correspondence to this author at UPSA Laboratoires, 128 rue Danton, 92506 Rueil-Malmaison, France [telephone (33) 1.47.16.86.00; fax (33) 1.47.16.89.97].

® Abstract published in *Advance ACS Abstracts,* December 15, 1996.

S1043-1802(96)00076-6 CCC: $14.00

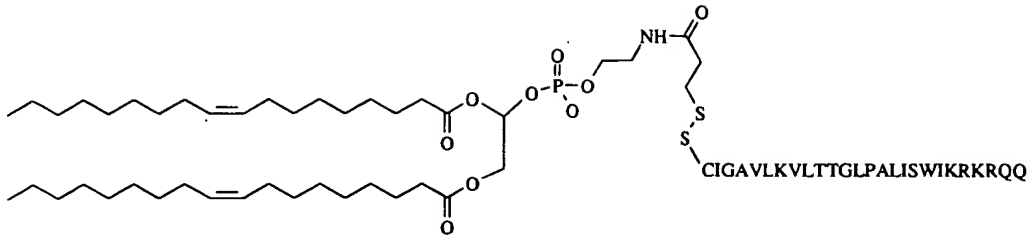

Figure 1. Structure of dioleoylmelittin.

phase HPLC, and the molecular weight was determined by ionization spray positive mode mass spectrometry: M = 2892.6 $(M + H)^+$ (calculated 2892.6 for $C_{132}H_{231}N_{39}O_3S$). Ten micromoles of compound **I** was dissolved in a mixture of 1 mL of 100 mM phosphate buffer (pH 6.5) and 1 mL of acetonitrile (*15*). Eleven micromoles of 1,2-dioleoyl-*sn*-glycero-3-phosphoethanolamine-*N*-[3-(2-pyridyldithio)-propionate] (N-PDP-PE, Avanti Polar Lipids Inc., Birmingham, AL) in 2.8 mL of chloroform was then added. The mixture was left at room temperature for 1 h, and the organic solvent was removed by evaporation under nitrogen. The remaining solution was diluted with distilled water to a volume of 2.5 mL and passed through a Sephadex G-25 M column. The resulting lipopeptide, dioleoylmelittin (Figure 1), was eluted with distilled water and lyophilized, yielding 28.9 mg of a white solid. The molecular weight was determined by ionization spray positive mode mass spectrometry: M = 3722 (calculated 3722.7 for $C_{176}H_{311}N_{40}O_{40}PS_2$).

A control peptide resulting from the coupling of NPDP-PE with CKKKKK (dioleoyl-K_5) was prepared as above, yielding 60 mg of purified lyophilisate (M = 1633.0, calculated 1633.25 for $C_{79}H_{150}N_{13}O_{16}S_2$).

Hemolysis Test. Blood from beagle dogs was collected on lithium heparinate and centrifuged for 20 min at 1000*g*. Plasma and buffy coat were discarded, and red blood cells (RBC) were washed with isotonic saline and finally diluted to a concentration of about 6×10^8 cells/mL. Melittin (Sigma, St. Louis, MO; sequencing grade) or dioleoylmelittin, complexed or not with plasmid DNA at a 2/1 +/− charge ratio (assuming a charge of +5 for each peptide), was sequentially diluted with isotonic saline from 40 to 0.05 μM in a 96-well plate. One hundred microliters of the RBC suspension was added per well, and the plate was incubated for 30 min at 37 °C. After centrifugation (15 min, 1000*g*), 80 μL of each supernatant was transfered to a new 96-well plate and hemoglobin concentration was measured using a hemoglobin diagnostic kit (Roche diagnostic). Two hundred microliters of a 0.77 mM potassium cyanide solution was added per well, and after 10 min, absorbance was read at 560 nm using an ELISA plate reader. One hundred percent hemolysis was obtained by incubating the RBC with 1% Triton X-100. Background was measured after the RBC had been incubated in isotonic saline and was subtracted from each value.

Destabilization of Liposomes. Egg phosphatidylcholine liposomes (Lipoïd, Ludwigshafen, Germany) were prepared by drying the lipids from a chloroform solution under vacuum and by rehydrating the lipid film with isotonic saline. Liposomes were then sonicated and extruded through polycarbonate filters with decreasing pore size (1, 0.4, 0.2 μm) to generate liposomes with an apparent diameter of 203 ± 4 nm (*16*). Liposomes, at a final concentration of 1mM in isotonic saline, were then incubated with increasing concentrations (from 5 to 140 μM) of melittin or dioleoylmelittin. Five minutes after addition of the peptide to the liposomes, the modification of the apparent diameter and the polydispersity of the liposomes was determined by dynamic light scattering (Zetasizer 4, Malvern Instruments, Southborough, MA).

Expression Vectors. The pGL3-CMV plasmid encoding for luciferase was constructed as follows: in a first step the *Kpn*I−*Bgl*II TK promoter fragment from pT109luc (*17*) was introduced between the *Kpn*I and *Bgl*II sites of pGL3basic (Promega, Madison, WI), respectively. From this construct the *Xho*I−*Bgl*II TK promoter was replaced by the CMV promoter excised as a 788 bp *Xho*I−*Bam*HI fragment from pUHD10-1 (*18*), generating pGL3-CMV. The pCMV-βgal plasmid encoding for β-galactosidase was purchased from Clontech (Palo Alto, CA). Both plasmids were grown using standard methods and purified by column chromatography (Qiagen, Hilden, Germany).

Preparation of the Transfecting Complex. Dioleoylmelittin was dissolved in trifluoroethanol at a concentration of 1 mg/mL. One milliliter of the solution was dried under argon and then under high vacuum. The film was dissolved with 1 mL of 10 mM Tris maleate buffer (pH 6), and the solution was vortexed. Typical complex was prepared by diluting 10 μg of plasmid DNA in a final volume of 200 μL of sterile water in a polystyrene tube. Then, an appropriate amount (typically 100 μL) of dioleoylmelittin was added dropwise and quickly mixed. The complex was allowed to stand at room temperature for 2−5 min before transfection. In some experiments, dioleoylmelittin was mixed with a 5-fold molar excess of DOPE (Avanti Polar Lipids) and subsequently added to plasmid DNA. The transfection efficiency of dioleoylmelittin was also compared to that of 1,2-bis(oleoyloxy)-3-(trimethylammonio)propane (DOTAP; Avanti Polar Lipids) and 1,3-dioleoyloxy-2-(6-carboxyspermyl)propylamide (DOSPER; Boehringer-Mannheim, Mannheim, Germany). DOTAP/DNA or DOSPER/DNA complexes were prepared according to the manufacturer's instructions and were used at a cationic liposome/DNA ratio of 5/1 (w/w). This corresponds to a 2/1 and 5/1 +/− cationic liposome/DNA charge ratio for DOTAP and DOSPER, respectively. The mean diameter of DOTAP/DNA and DOSPER/DNA complexes was 190 ± 10 nm, as determined by dynamic light scattering.

Transfection Experiments. CV-1 (monkey kidney fibroblasts) cells were plated at a density of about 2×10^4 cells per well in a 96-well plate (about 70−80% confluency) and grown for 24 h in 10% fetal calf serum (FCS, Gibco BRL, Grand Island, NY) containing medium. Transfection took place in 100 μL of FCS-free Dulbecco's modified Eagle medium (DMEM), and 5 h later medium was removed and replaced by 10% FCS-containing medium. To each well was applied 0.2 μg of plasmid DNA. In some experiments, transfection took place in 10% or 50% FCS-containing medium. Forty-eight hours later, β-galactosidase activity was measured. After medium removal, 50 μL of 250 mM Tris Cl buffer (pH 8) containing 0.5% of Triton X-100 was added per well. Cells were frozen at −70 °C and then thawed at 37 °C, and 50 μL of phosphate buffer saline (150 mM, pH 6, PBS) was added

per well. Finally, 150 μL of a 2 mg/mL solution of *o*-nitrophenyl galactopyranoside (Sigma) in 60 mM Na_2HPO_4, 1 mM $MgSO_4$, 10 mM KCl, and 50 mM β-mercaptoethanol was added per well. Optical density at 405 nm was measured after the plate was incubated for anywhere between 20 min and 1 h at 37 °C, depending on the β-galactosidase activity. Values were computed from a β-galactosidase (Fluka) standard curve. Day-to-day β-galactosidase activity values usually varied by about 2-fold depending upon cell density and condition of the cells. Sensitivity of the assay was 50 μunits of β-galactosidase per well of CV-1 cells.

β-Galactosidase activity was also detected by cytochemical stain to evaluate the percentage of transfected cells (*19*). In this case, CV-1 cells and primary rabbit aorta smooth muscle cells (*20*) were grown in 60 mm dishes in 2 mL of appropriate medium. Two micrograms of pCMVβgal plasmid complexed with 20 μg of dioleoylmelittin was incubated with the cells during 5 h in 2 mL of serum-free medium. Forty-eight hours after tranfection, cells were rinsed with PBS, fixed for 5 min with 4% formaldehyde in PBS, and then stained with X-Gal (5-bromo-4-chloro-3-indolyl-β-D-galactoside, Promega). The blue β-galactosidase-expressing cells were visualized under the microscope 2 h after staining and counted as the percentage of the total cell population.

The dioleoylmelittin transfection efficiency was also compared to that of cationic liposomes (DOTAP or DOSPER), and in this case a luciferase expression vector, pGL3-CMV, was used. Cell-lines CV-1, CHO-K1 (Chinese hamster ovary cells), and 293 (human kidney embryonic cells) were plated in six-well plates and grown for 24 h. Two micrograms of DNA complexed with either cationic liposomes or dioleoylmelittin was added per dish in 2 mL of 10% FCS-containing medium. Five hours later medium was removed and replaced by fresh 10% FCS-containing medium. Luciferase activity was measured 48 h later as previously described (*21*), and results were normalized to cell protein content (BCA protein assay reagent, Pierce, Rockford, IL).

Physicochemical Characterization. Size and zeta potential of the dioleoylmelittin/DNA complex were determined using a Zetasizer 4 (Malvern Instruments) after appropriate dilution in pure water. To estimate the interaction between plasmid DNA and dioleoylmelittin, plasmid DNA (0.5 μg) was mixed with increasing amounts of dioleoylmelittin (0−4 μg) and electrophoresed on a 0.8% agarose gel in the presence of ethidium bromide. Dioleoylmelittin/DNA complex was also imaged by electron microscopy (EM). For negative staining, a 5 μL aliquot of sample was adsorbed to a carbon-coated 200-mesh copper grid. Staining was done by adding directly 10 μL of 2% uranyl acetate to the adsorbed sample droplet, and the preparation was air-dried after removal of the excess of liquid with filter paper. Specimens were examined in a JEOL-1210 electron microscope operated at 100 kV. For cryoelectron microscopy of frozen−hydrated specimens, 5 μL of samples was applied to 700-mesh hexagonal copper grids. After the excess of solution was removed by blotting with filter paper, the grid was rapidly quench-frozen in a home-made guillotine-like device using liquid ethane as coolant. The frozen grids were mounted under liquid nitrogen in a side entry specimen holder (Model 626, Gatan, Pleasanton, CA) and examined at −172 °C in a JEOL-1210 electron microscope equipped with a anticontaminator (Model TAC100, Oxford Instruments, Oxon, U.K.) and operated at 100 kV. Low-dose images were recorded 1.5−2.0 μ underfocus with an electron irradiation of approximately 10 e/Å^2 at a nominal magnification of 10 000−20 000. Digitized micrographs were recorded with a slow scan CCD camera (Model 679, Gatan). Magnification calibration was done using negatively stained catalase crystals.

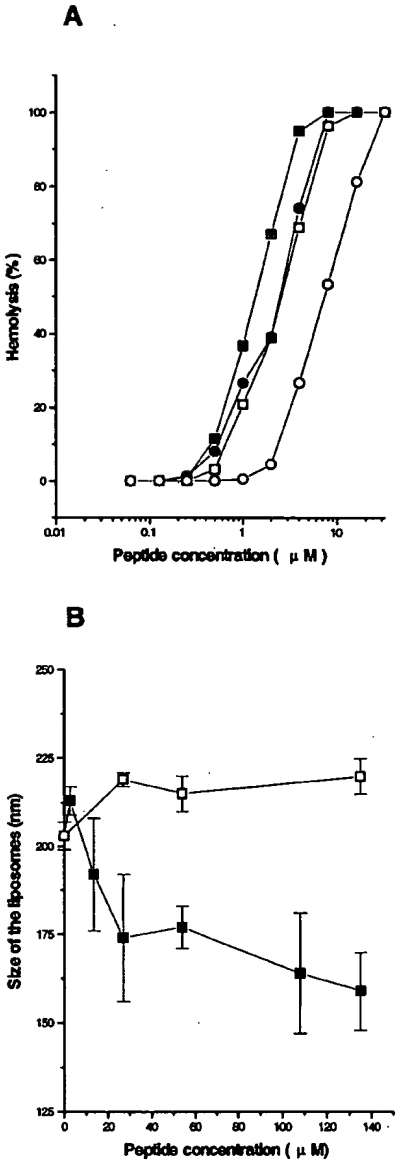

Figure 2. Hemolytic activity (A) and liposome-destabilizing activity (B) of melittin (■), melittin/DNA complex (●), dioleoylmelittin (□), and dioleoylmelittin/DNA complex (○). Complexes between peptides and DNA were prepared at a 2/1 (+/−) charge ratio, assuming 5 positive charges for each peptide.

RESULTS

Membrane-Disturbing Activity of Melittin and Dioleoylmelittin Complexed or Not with Plasmid DNA. Two tests were used to evaluate the membrane-disturbing activity of dioleoylmelittin, as compared to melittin: the hemolytic activity and the solubilization of liposomes. When free melittin was incubated with erythrocytes at 37 °C, 50% hemolysis could be detected at a peptide concentration of about 1.2 μM (Figure 2A). This concentration doubled when melittin was complexed with plasmid DNA. Dioleoylmelittin had a lower hemolytic activity than the original peptide, and 50% hemolysis was attained at a peptide concentration of 2.5 μM. After complexation with DNA, the dioleoylmelittin concentration that induced 50% hemolysis was 7 μM. At a

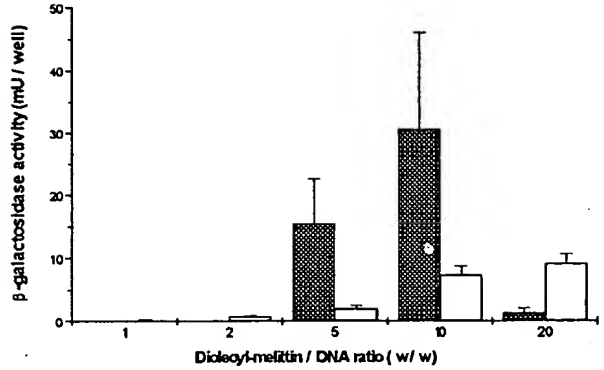

Figure 3. Effect of dioleoylmelittin/DNA ratio (w/w) on transfection efficiency of CV-1 cells in the presence (open bar) or absence (black bar) of DOPE in the complex. Results are the mean ± SD of six wells in two separate experiments.

concentration of 5 μM, melittin slightly increased the size of egg PC liposomes, but at concentrations above 10 μM, it markedly decreased their size and increased their polydispersity (Figure 2B). This effect was attributed to the fusion of liposomes at low peptide/lipid ratios followed by the solubilization of the liposomes and the formation of discoidal structures at higher melittin concentrations (*22*). Conversely, dioleoylmelittin only slightly increased the size of the liposomes and did not modify their polydispersity in the range of concentration studied.

***In Vitro* Transfection with the Dioleoylmelittin/DNA Complex.** The optimal dioleoylmelittin/DNA ratio for transfection of CV-1 cells was first determined (Figure 3). At a 1/1 or 2/1 dioleoylmelittin/DNA ratio (w/w), no transfection was detected. However, when the dioleoylmelittin/DNA ratio was at least 5/1 (w/w), β-galactosidase activity could be detected in CV-1 cells 48 h after transfection and the optimal dioleoylmelittin/DNA ratio was 10/1 (w/w). Above this ratio some toxicity appeared and transfection was reduced. When DOPE was added to the transfecting particles in a 5-fold molar excess to dioleoylmelittin, β-galactosidase activity was induced at dioleoylmelittin/DNA ratios at which DOPE-free formulations hardly mediated transfection. However, at the optimal ratio with DNA, the efficiency of the DOPE-containing formulations was reduced 5−10-fold as compared to the dioleoylmelittin alone. Furthermore, the control peptide dioleoyl-K_5 did not mediate any transfection of CV-1 cells at all lipopeptide/DNA ratios studied (data not shown).

Evaluation of the percentage of cells expressing β-galactosidase activity by cytochemical staining indicated that about 60−70% and 10−20% of the cells were transfected for CV-1 cells and primary rabbit aorta smooth muscle cells, respectively (data not shown).

The transfection efficiency of dioleoylmelittin was also compared to that of two commercially available cationic lipid transfection reagents, DOTAP and DOSPER, in various cell lines (Table 1). In the three cell lines studied, dioleoylmelittin mediated 3−40 and 25−500 times greater luciferase activity than DOSPER and DOTAP, respectively.

Effect of Serum and Lysomotrophic Agents on Transfection Efficiency. Surprisingly, the presence of FCS in the medium had a favorable effect on the transfection efficiency of dioleoylmelittin in CV-1 cells (Figure 4). Ten percent FCS in the transfection medium slightly enhanced transfection, but 50% FCS enhanced β-galactosidase activity more than 2-fold. This effect was not cell line dependent since an improvement of transfection in the presence of serum was also observed for

Table 1. Transfection of Various Mammalian Cell Lines with Dioleoylmelittin Complex or Cationic Lipids

	luciferase activity[a]		
	DOTAP	DOSPER	dioleoylmelittin
CHO-K1	2.69×10^6	2.50×10^7	5.19×10^8
CV-1	1.14×10^5	1.31×10^6	5.54×10^7
293	7.31×10^6	5.70×10^7	1.71×10^8

[a] Results are expressed as light units per milligram of cell protein and are the mean of two experiments. Background (130 LU) was subtracted from each measurement.

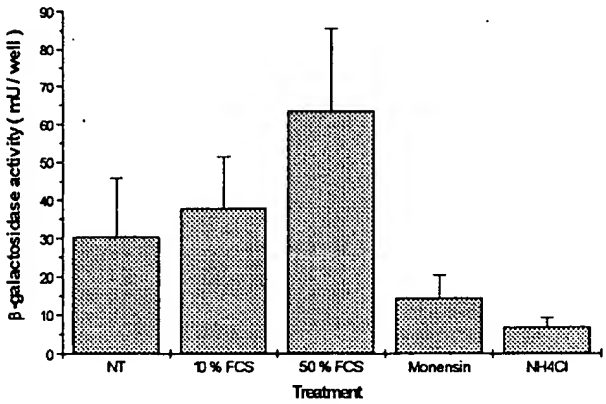

Figure 4. Effect of various agents on dioleoylmelittin-mediated transfection. NT, no treatment. Results are the mean ± SD of at least 10 wells in three separate experiments..

293 or COS-1 cells (data not shown). Furthermore, cell viability was at least 96% in the absence or the presence of serum, suggesting that FCS did not improve transfection by protecting the cells from a possible toxic effect of the dioleoylmelittin.

To gain some insight into the mechanism whereby dioleoylmelittin brings about transfection, cells were also treated with various agents during the transfection procedure (Figure 4). Addition of lysomotrophic agents, monensin (10 μM) and ammonium chloride (20 mM), at the beginning of the 5 h incubation time reduced 2−3 times the transfection level mediated by the dioleoylmelittin. These compounds have been shown to enhance cationic lipid-mediated transfection in CV-1 cells (*23*).

Characterization of the Dioleoylmelittin/DNA Complex. Rehydration of the dioleoylmelittin film resulted in a clear solution. Under negative-stain EM this solution appeared as aggregates or micellar-like structures with a size between 5 and 10 nm (Figure 5a).

Dynamic light scattering indicated that homogeneous particles with an apparent diameter of about 170 nm were formed when dioleoylmelittin was added to DNA at a weigth ratio between 2 and 4 (Figure 6). When increasing amounts of dioleoylmelittin were added, the mean size of the complex slightly increased to 250 nm. Addition of DOPE to the dioleoylmelittin/DNA complex led to less homogeneous particles of a size larger than 400 nm (data not shown). Zeta potential measurements showed that when dioleoylmelittin was added to the DNA solution, particles became more and more positive. Charge neutralization (zeta potential between −1 and +1 mV) was obtained at a dioleoylmelittin/DNA ratio between 4/1 and 8/1 (w/w) (Figure 6). Similarly, gel electrophoresis showed that plasmid DNA was completely retained in the agarose gel when mixed at a dioleoylmelittin/DNA weigth ratio above 4/1 (data not shown). This finding was in good agreement with zeta potential measurements.

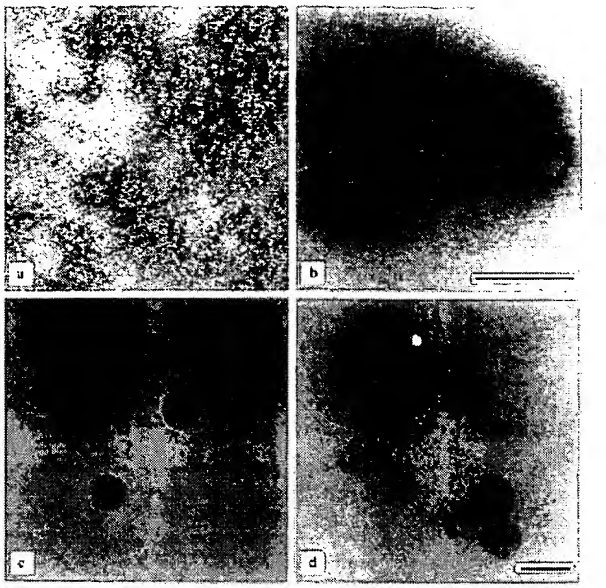

Figure 5. Electron micrographs of negative-stained (a, b) or frozen–hydrated (c, d) samples: dioleoylmelittin (a), dioleoylmelittin/DNA 10/1 (w/w) complex (b, d), and dioleoylmelittin/DNA 2/1 (w/w) complex (c). Bars represent 200 nm and are the same for (a) and (b) and for (c) and (d).

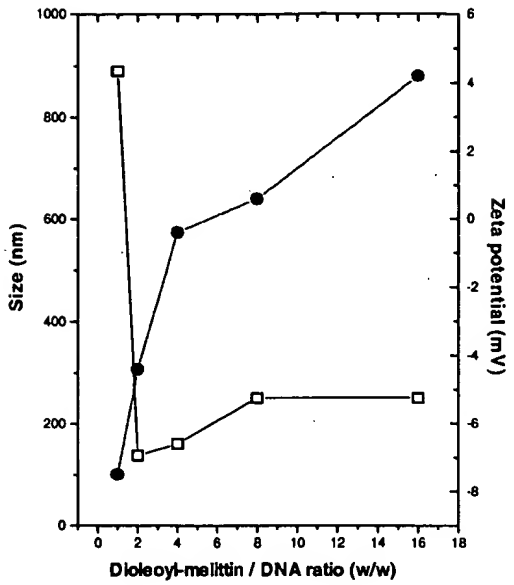

Figure 6. Evolution of the mean size (□) and the mean zeta potential (●) of the particles as a function of the dioleoylmelittin/DNA ratio (w/w).

The dioleoylmelittin/DNA complex was also imaged by negative-stain EM and cryo-EM (Figure 5). At a 2/1 dioleoylmelittin/DNA weight ratio, spherical, filled particles with diameters between 50 and 150 nm were visualized under cryo-EM (Figure 5c). No aggregates or large structures were seen in any sample. Similar structures were observed for the 10/1 dioleoylmelittin/DNA complex (w/w), although particles larger than 200 nm were sometimes visualized in the sample (Figure 5d). Negative-stain EM revealed similar structures as for cryo-EM, albeit aggregated particles were seen more frequently (Figure 5b). These results confirmed the data obtained by laser light scattering.

DISCUSSION

Conjugation of 1,2-dioleoylphosphatidylethanolamine-*N*-[3-(2-pyridyldithio)propionate] with [Cys^1]melittin resulted in a hybrid molecule, the dioleoylmelittin, with properties different from those of the native peptide melittin. Indeed, although melittin binds DNA by charge interactions, the melittin/DNA complex does not mediate transfection and, due to the fast partitioning of melittin into cell membranes, induces high toxicity (*8*). In contrast, dioleoylmelittin was able to complex plasmid DNA to form homogeneous and small particles. The resulting dioleoylmelittin/DNA complex mediated efficient transfection of various cell types *in vitro*, including primary cells.

Dioleoylmelittin in aqueous solution forms aggregates that resemble micellar structures rather than liposomes. This characteristic distinguishes dioleoylmelittin from cationic lipids which spontaneously form liposomes in aqueous solution (*24*, *25*). Unlike dioleoylmelittin/DNA complexes, cationic lipid/DNA complexes often appear as heterogeneous structures in EM (*25*–*27*). Recently, it has been shown that complexation of DNA with cationic lipids in a micellar state followed by dialysis of the preparation to remove the surfactant allowed the formation of small and stable particles (*28*). Therefore, due to a higher molecular motion, cationic amphiphiles in a micellar-like state could interact more favorably with plasmid DNA than in a liposomal state (*29*).

The highest transfection of CV-1 cells was obtained for a 10/1 dioleoylmelittin/DNA ratio (w/w), which corresponds to a theoretical 5/1 +/− charge ratio, assuming 5 positive charges for dioleoylmelittin. The particles formed at this ratio had a net positive charge (zeta potential of 1.2 mV) and, as indicated by DNA gel electrophoresis, plasmid DNA was totally complexed by dioleoylmelittin. The absence of other structure in negative-stain EM or cryo-EM indicates that these particles are likely to be responsible for transfection.

Unlike other amphipathic molecule-based transfection systems, dioleoylmelittin did not require DOPE to mediate transfection (*3*, *4*, *8*). In contrast, at the optimal dioleoylmelittin/DNA ratio, addition of DOPE increased particle size and transfection efficiency decreased. Another interesting feature of the dioleoylmelittin system is its ability to mediate high transfection in the presence of serum. This is also in contrast to other transfection reagents such as cationic liposomes or the gramicidin S/DNA/DOPE complex for which 50% FCS in the transfection medium dramatically reduces transfection efficiency (*8*). This property should make dioleoylmelittin an attractive transfection reagent for serum-sensitive cell lines. Nevertheless, the reason FCS increases transfection is still unknown. The formation of small, compacted structures is undoubtely an important feature to mediate high transfection in the presence of serum, as shown for cationic lipid- or polylysine-based systems (*28*, *30*). However, other factors such as complement activation may be involved in the enhancement of dioleoylmelittin transfection efficiency by serum (*31*). We are currently investigating this possibility.

The cationic nature of the melittin moiety was necessary but not sufficient to mediate high levels of transfection. Indeed, replacement of the melittin by an oligolysine of five residues completely abolished transfection. Although high molecular weight polylysine covalently coupled with phosphatidylethanolamine can mediate transfection of cells in culture, scraping of the cells or addition of a helper lipid is required for efficient gene transfer with this reagent (*32*, *33*). This indicates that the entry of DNA into cells and/or lysosomal escape using lipopolylysine is poor, which is due to the fact that

polylysine has no or limited membrane-disturbing activity. In contrast, both melittin and dioleoylmelittin can destabilize membranes, as shown by their ability in lysing red blood cells. However, melittin and dioleoylmelittin have somewhat different behaviors regarding their action on membranes. Dioleoylmelittin did not solubilize liposomes at concentrations below 140 μM, and the concentration that induced hemolysis was about 2−3-fold higher than that of melittin. This could explain why dioleoylmelittin, in contrast to melittin, did not induce cell toxicity at the concentrations used for transfection ($\leq$5 μM).

Treatment of the cells with lysomotrophic agents during the transfection procedure decreased 2−3-fold the level of β-galactosidase expression. This observation suggests that DNA delivery using dioleoylmelittin may involve an endosomal/lysosomal pathway (*23*). Cationic lipid/DNA complexes also enter the cell by endocytosis (*23*, *34*). Xu and Szoka have recently proposed that after endocytosis of the cationic lipid/DNA complex, destabilization of the early endosome occurs followed by a flip-flop of the anionic phospholipids of the endosomal membrane (*35*). Then, these anionic lipids diffuse into the complex to form ion pairs with cationic lipids, leading to the displacement of plasmid DNA from the transfecting complex. In the case of dioleoylmelittin, such a mechanism may also be possible since melittin can induce a rapid and extensive lipid flip-flop in membranes (*36*). Furthermore, the affinity of melittin for membrane-containing anionic lipids is 100-fold greater than for zwitterionic lipids (*12*). However, in contrast to cationic lipids for which lysomotrophic agents usually increase gene transfer efficiency (*23*), dioleoylmelittin transfection efficiency was decreased when monensin or ammonium chloride were present during transfection. Nevertheless, the exact mechanism whereby dioleoylmelittin is mediating transfection is still unresolved. In particular, it is unclear whether dioleoylmelittin is the actual transfecting agent or if it acts as a prodrug that releases the more active melittin after reduction of the disulfide bridge.

The use of dioleoylmelittin for *in vivo* gene transfer, especially in humans, may be precluded by the immunogenic potential of the melittin (*37*). However, similar hybrid molecules based on membrane-disturbing, nonimmunogenic peptides could perhaps be engineered to deliver genes *in vivo*. In conclusion, dioleoylmelittin represents a new class of efficient, *in vitro* transfecting reagent, especially suited for serum-sensitive cells.

ACKNOWLEDGMENT

We are grateful to Dr. J. Fingerle (F. Hoffmann-La Roche) for providing rabbit aorta smooth muscle cells. We greatly appreciate the expertise of Mrs. B. Hennequin in the dioleoylmelittin purification.

LITERATURE CITED

(1) Knowles, M. R., Hohneker, K. W., Zhou, Z., Olsen, J. C., Noah, T. L., Hu, P. C., Leigh, M. W., Engelhardt, J. F., Edwards, L. J., Jones, K. R., Grossman, M., Wilson, J. M., Johnson, L. G., and Boucher, R. C. (1995) A controlled study of adenoviral-vector-mediated gene transfer in the nasal epithelium of patients with cystic fibrosis. *N. Engl. J. Med. 333*, 823−831.

(2) Ledley, F. D. (1995) Nonviral gene therapy: the promise of genes as pharmaceutical products. *Hum. Gene Ther. 6*, 1129−1144.

(3) Behr, J. P. (1994) Gene transfer with synthetic cationic amphiphiles: prospects for gene therapy. *Bioconjugate Chem. 5*, 382−389.

(4) Gao, X., and Huang, L. (1995) Cationic liposome-mediated gene transfer. *Gene Ther. 2*, 710−722.

(5) Wagner, E., Plank, C., Zatloukal, K., Cotten, M., and Birnstiel, M. (1992) Influenza virus hemagglutinin HA-2 N-terminal fusogenic peptides augment gene transfer by transferrin-polylysine-DNA complexes: toward a synthetic virus-like gene transfer vehicle. *Proc. Natl. Acad. Sci. U.S.A. 89*, 7934−7938.

(6) Haensler, J., and Szoka, F. C. (1993) Polyamidoamine cascade polymers mediate efficient transfection of cells in culture. *Bioconjugate Chem. 4*, 372−379.

(7) Plank, C., Oberhauser, B., Mechtler, K., Koch, C., and Wagner, E. (1994) The influence of endosome-disruptive peptides on gene transfer using synthetic virus-like gene transfer systems. *J. Biol. Chem. 269*, 12918−12924.

(8) Legendre, J. Y., and Szoka, F. C. (1993) Cyclic amphipathic peptide-DNA complexes mediate high efficiency transfection of adherent mammalian cells *Proc. Natl. Acad. Sci. U.S.A. 90*, 893−897.

(9) Legendre, J. Y., and Supersaxo, A. (1995) Short-chain phospholipids enhance amphipathic peptide-mediated gene transfer. *Biochem. Biophys. Res. Commun. 217*, 179−185.

(10) Hara, T., Kuwasawa, H., Aramaki, Y., Takada, S., Koike, K., Ishidate, K., Kato, H., and Tsuchiya, S. (1996) Effects of fusogenic and DNA-binding amphiphilic compounds on the receptor-mediated gene transfer into hepatic cells by asialofetuin-labeled liposomes. *Biochim. Biophys. Acta 1278*, 51−58.

(11) Kamata, H., Yagisawa, H., Takahashi, S., and Hirata, H. (1994) Amphiphilic peptides enhance the efficiency of liposome-mediated DNA transfection. *Nucleic Acids Res. 22*, 536−537.

(12) Dempsey, C. E. (1990) The actions of melittin on membranes. *Biochim. Biophys. Acta 1031*, 143−161.

(13) Atherton, E., and Sheppard, R. C. (1989) in *Solid Phase Peptide Synthesis: A Practical Approach* (D. Rickwoods and B. D. Hames, Eds.) IRL Press, Oxford, U.K.

(14) Knorr, R., Trzeciak, A., Bannwarth, W., and Gillessen, D. (1989) New coupling reagents in peptide chemistry. *Tetrahedron Lett. 30*, 1927−1930.

(15) Zuckermann, R., Corey, D., and Schultz, P. (1987) Efficient methods for attachment of thiol specific probes to the 3'-ends of synthetic oligodeoxyribonucleotides. *Nucleic Acids Res. 15*, 15305−15321.

(16) Olson, F., Hunt, T., Szoka, F. C., Vail, W. J., and Papahadjopoulos, D. (1979) Preparation of liposomes of defined size distribution by extrusion through polycarbonate membranes. *Biochim. Biophys. Acta 557*, 9−23.

(17) Nordeen, S. K. (1988) Luciferase reporter gene vectors for analysis of promoters and enhancers. *BioTechniques 6*, 454−458.

(18) Deuschle, U., Pepperkok, R., Wang, F. B., Giordano, T. J., McAllister, W. T., Ansorge, W., and Bujard, H. (1989) Regulated expression of foreign genes in mammalian cells under the control of coliphage T3 RNA polymerase and lac repressor. *Proc. Natl. Acad. Sci. U.S.A. 86*, 5400−5404.

(19) McGregor, G. R., Mogg, A. E., Burke, J. F., and Caskey, C. T. (1987) Histochemical staining of clonal mammalian cell lines expressing *E. coli* β galactosidase indicates heterogeneous expression of the bacterial gene. *Somat. Cell. Mol. Genet. 13*, 253−265.

(20) Owens, G. K., and Thompson, L. G. (1986) Expression of smooth muscle specific isoactin in cultured smooth muscle cells: relationship between growth and cytodifferentiation. *J. Cell Biol. 102*, 343−352.

(21) Brasier, A. R., Tate, J. E., and Habener, J. F. (1989) Optimized use of the firefly luciferase assay as a reporter gene in mammalian cell lines. *BioTechniques 7*, 1116−1122.

(22) Dufourcq, J., Faucon, J. F., Fourche, G., Dasseux, J. L., Le Maire, M., and Gulik-Krzywicki, T. (1986) Morphological changes of phosphatidylcholine bilayers induced by melittin: vesicularization, fusion, discoidal particles. *Biochim. Biophys. Acta 859*, 33−48.

(23) Legendre, J. Y., and Szoka, F. C. (1992) Delivery of plasmid DNA into mammalian cells using pH-sensitive liposomes: comparison with cationic liposomes. *Pharm. Res. 9*, 1235−1242.

(24) Felgner, P. L., Gadek, T. R., Holm, M., Roman, R., Chan, H. W., Wenz, M., Northrop, J. P., Ringold, G. M., and Danielsen, M. (1987) Lipofection: a highly efficient, lipid-mediated DNA transfection procedure. *Proc. Natl. Acad. Sci. U.S.A. 84*, 7413–7417.

(25) Gershon, H., Ghirlando, R., Guttman, S. B., and Minsky, A. (1993) Mode of formation and structural features of DNA-cationic liposome complexes used for transfection. *Biochemistry 32*, 7143–7151.

(26) Sternberg, B., Sorgi, F. L., and Huang, L. (1994) New structures in complex formation between DNA and cationic liposomes visualized by freeze-fracture electron microscopy. *FEBS Lett. 356*, 361–366.

(27) Gustafsson, J., Arvidson, G., Karlsson, G., and Almgren M. (1995) Complexes between cationic liposomes and DNA visualized by cryo-TEM. *Biochim. Biophys. Acta 1235*, 305–312.

(28) Hofland, H. E. J., Shephard, L., and Sullivan, S. M. (1996) Formation of stable cationic lipid/DNA complexes for gene transfer. *Proc. Natl. Acad. Sci. U.S.A. 93*, 7305–7309.

(29) Behr, J. P. (1986) DNA strongly binds to micelles and vesicles containing lipopolyamines or lipointercalants. *Tetrahedron Lett. 27*, 5861–5864.

(30) Vitiello, L., Chonn, A., Wasserman, J. D., Duff, C., and Worton, R. G. (1996) Condensation of plasmid DNA with polylysine improves liposome-mediated gene transfer into established and primary muscle cells. *Gene Ther. 3*, 396–404.

(31) Plank,C., Mechtler, K., Szoka, F. C., and Wagner E. (1996) Activation of the complement system by synthetic DNA complexes: a potential barrier for intravenous gene delivery. *Hum. Gene Ther. 7*, 1437–1446.

(32) Zhou, X., Klibanov, A. L., and Huang, L. (1991) Lipophilic polylysines mediate efficient DNA transfection in mammalian cells. *Biochim. Biophys. Acta 1065*, 8–14.

(33) Zhou, X., and Huang, L. (1994) DNA transfection mediated by cationic liposomes containing lipopolylysine: characterization and mechanism of action. *Biochim. Biophys. Acta 1189*, 195–203.

(34) Zabner, J., Fasbender, A. J., Moninger, T., Poellinger, K. A., and Welsh, M. J. (1995) Cellular and molecular barriers to gene transfer by a cationic lipid. *J. Biol. Chem. 270*, 18997–19007.

(35) Xu, Y., and Szoka, F. C. (1996) Mechanism of DNA release from cationic liposome/DNA complexes used in cell transfection. *Biochemistry 35*, 5616–5623.

(36) Fattal, E., Nir, S., Parente, R. A., and Szoka, F. C. (1994) Pore-forming peptides induce rapid phospholipid flip-flop in membranes. *Biochemistry 33*, 6721–6730.

(37) Kemeny, D. M., McKenzie-Mills, M., Harries, M. G., Youlten, L. J. F., and Lessof, M. H. (1983) Antibodies to purified bee venom proteins and peptides. *J. Allergy Clin. Immunol. 72*, 376–385.

BC960076D

NO 6/15

STIC-ILL

From: Schnizer, Richard
Sent: Tuesday, June 15, 2004 1:13 PM
To: STIC-ILL
Subject: 09/555,574

499892

Please send me a copy of :

Radley et al (Molecular Crystals and Liquid Crystals Science and Technology, Section A: Molecular Crystals nad Liquid Crystals (1997), 303: 249-254 0026-8941

Ziady et al (Am. J. Physiol. (197) 273(2, part 1): G545-G552)

Legendre et al (Bioconj. Chem. (1997) 8(1): 57-63)

Washwa et al (Bioconjugate Chemistry (1997) 8(1): 81-88

Thank you-

Richard Schnizer, Ph.D.
Patent Examiner
Art Unit 1635
Remsen 2C01
571-272-0762
Mail Box 2C18

14254212-NC

CAI
6/16

Mol. Cryst. Liq. Cryst., 1997, Vol. 303, pp. 249–254
Reprints available directly from the publisher
Photocopying permitted by license only

THE USE OF THE DECYL ESTERS OF AMINO ACID HYDROCHLORIDES AS CHIRAL DOPANTS IN THE FORMATION OF AMPHIPHILIC CHOLESTERIC LIQUID CRYSTALS

K RADLEY*, N McLAY and K GICQUEL
Department of Chemical and Biological Sciences The University of Huddersfield
Queensgate Huddersfield HD1 3DH ENGLAND

Abstract The decyl ester hydrochlorides of the amino acids serine, alanine, leucine, methionine and methyl cysteine are accessed as chiral dopants in amphiphilic cholesteric liquid crystal formation. The sense and magnitude of the induced helical twist is found to be dependent on the achiral host detergent, which were various alkyl-methyl ammonium bromide salts. The results are interpreted in terms of the trans and cis rotamers associated with the ester linkage. ^{13}C-NMR is used to measure the rotamer populations. Each rotamer makes an opposite but an unequal contribution to the total twist. The results for the serine ester did not fit this interpretation completely.

INTRODUCTION

Micellar nematics are orientationally ordered lyotropic liquid crystals formed by solvating or heating dimensionally ordered liquid crystals. Dimensionally ordered lamella and middle soap phases are associated with cylindrical and disk shaped micelles respectively.[1] It was found that when chiral dopants were added to micellar cholesteric states were formed.[2] The chiral center in cholesteric liquid crystal facilitates a spontaneously twist helical structures characterized as a repeat distance called the pitch. The twist is the inverse of the pitch. The twisting power is the differential of the twist inrespect to the concentration extrapolated to the origin. In the present study the ACHIRAL HOST DETERGENTS will be alkyl methyl ammonium bromides mixed with decanol and water:-$C_{14}H_{29}(CH_3)_3N^+Br^-$ (TDTMABr); $C_{12}H_{25}(CH_3)_2NH^+Br^-$ (DoDMABr); $C_{12}H_{25}(CH_3)NH_2^+Br^-$ (DoMABr) and $C_{10}H_{21}NH_3^+Br^-$ (DMABr).

Amino acids can be used as convenient sources of chiral centres in the synthesis of chiral dopants, ie. as precursors to esters and amide chiral detergent derivatives. It has been shown recently in the case of acylated (amide potassium salts) amino acids, that there is a strong relationship between the molecular stereochemistry and bulk chirality in amphiphilic cholesteric liquid crystals.[3] The acylated amino acids derived from primary

nitrogens in all cases gave rise to cholesteric states with the same sense of helical twist. In two cases proline and thiaproline, derived from secondary nitrogens, with the host detergent potassium laurate the sense of the helical twist was reversed. This reversal in the sense of the helical twist was explained in terms of trans and cis rotamers in which each rotamer makes an opposite in sense and not necessarily equal in magnitude contribution, to the total twist. This explaination was backed up by ^{13}C NMR, which facilitates the measurement of the rotamer populations.

Trans-cis rotamerisation is a well known phenomenon in peptide chemistry. Barriers of rotation in amides have been extensively studied using NMR since the 1960's[4].

The decyl ester hydrochloride of alanine has been used previously as a chiral host, which resulted in smaller twists than in the corresponding amides[5]. The decyl ester hydrochloride of proline has been used as a chiral dopant, where a concentration dependent reversal in twist sense was observed[6]. This phenomenon was explained in terms of trans-cis rotamers, where the rotamer populations were determined by ^{13}C NMR.

There is a less extensive literature for the ester rotamers than the amide rotamers. Rotamerisation in methyl formate has been studied both theoretical and experimentally[7,8]. Ester rotamers are thought to play a role as an inhibitor in the hydrolysis of β lactam esters(penicillic)[9].

Inversions in chirality have been observed in chiral thermotropic systems such as the phenyl esters[10].

EXPERIMENTAL

The chiral detergents were synthesized as previously described by passing HCl through the amino-acid refluxing in decanol[5]. The amino-acids chiral precursors were:- SERINE, ALANINE, LEUCINE, METHYL-CYSTEINE and METHIONINE.

The magnitudes of the helical twists was determined using laser diffraction through Bragg's law and using a polarizing microscope through observing fingerprint textures.

The sense of the helical twist is by convention opposite to the sign of the optical rotation.

$$\Theta = -2\pi Pd(\Delta n/\lambda)^2$$

The sign of the optical rotation could be determined in two ways.

(a) By mixing samples containing different chiral dopants and then checking the magnitude of the resulting helical twist for compensation or reinforcement.

(b) By optical microscopy through the observation of Grandjean textures and Cano wedges.

^{13}C NMR was taken with long acquisition times in order to obtain quantitative spectra for cis and trans rotamer population determination.

RESULTS and DISCUSSION

When the achiral host was tetradecyl-trimethyl ammonium bromide $C_{14}H_{29}(CH_3)_3N^+Br^-$ TDTMABr\ decanol\ water(CsCl), all the twisting powers produced by the chiral dopants were positive except the serine ester case. Whereas when the achiral host was decyl ammonium bromide $C_{10}H_{21}NH_3^+Br^-$ DABr\water\(NH_4Cl), all the twisting powers were negative including the serine ester case. It was attempted to acquire more results before any reasonable explanation might be put forward. The two more of the less well known alkyl methyl ammonium bromide detergent were investigated. When the host was dodecyl-dimethyl ammonium bromide $C_{12}H_{25}(CH_3)_2NH^+Br^-$ DoMABr\decanol\water (KCl) the twisting powers were negative in all cases except the serine ester case. Investigation with the host dodecyl methyl ammonium bromide $C_{12}H_{25}(CH_3)NH_2^+Br^-$ DoDMABr could not be made as the detergent at this time was unavailable.

TABLE :-Twisting powers cm^{-1} determined for various achiral hosts and chiral dopants

	DABr	DoDMABr	TMABr
DESCl	-3,200	+750	-2,100
DEMCl	-13,500	-1,950	+1,650
DEACl	-10,600	-850	+600
DEMCCl	-15,700	-1,000	+380
DEAL	-21,100	-5,000	+4,400

The data for the case of the decyl ester alanine hydrochloride DEACl, illustrated by plotting the twist as a function of dopant concentration (see figure I) was processed using microsoft origin, where the twisting power in each case was the slope of the line extrapolated through the origin, where the error was about 10%.

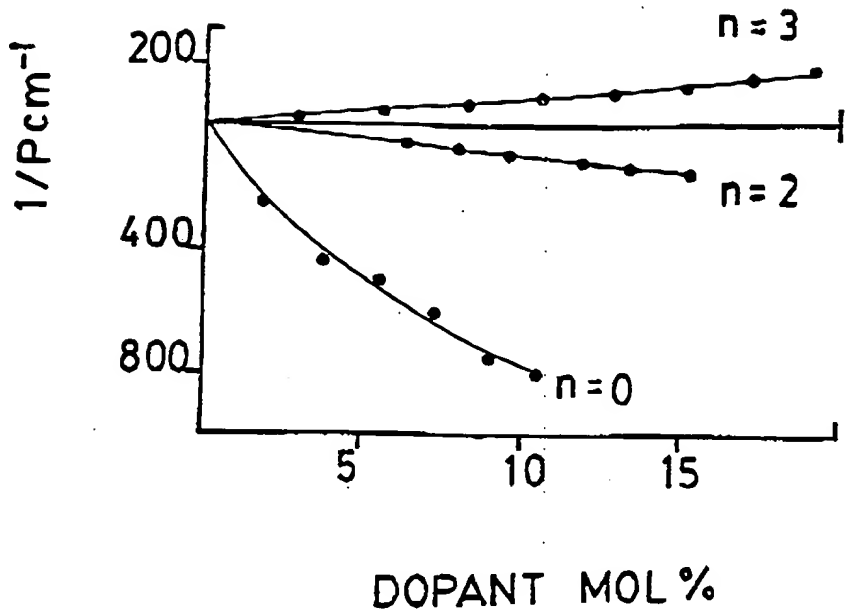

FIGURE I :-**The twist data derived from the chiral dopant DEACI (alanine) plotted as a function of dopant mol% for three alkyl methyl ammonium bromide host detergents, where n denotes the number of methyl groups in the ammonium headgroup @ 25 °C.**

If the basic assumption concerning the generation of the twist in an ACLC is that the total bulk twist is equal to the sum of the individual micro-twists, the following equation could be derived for the total twisting power T_T.

$$T_T = T_A + M_B (T_B - T_A)$$

where T_A and T_B are the individual twisting powers of rotamer A and B respectively and M_B is the fraction of rotamer B. It was assumed within experimental error that the magnitudes of T_A and T_B are independent of the achiral host and there is no inter doping chiral interactions. The populations of the trans and cis rotamers were calculated from the ^{13}C NMR data, hence M_B could be calculated. The twisting power data was plotted as a function of M_B, and was then fitted to a linear progression based on the above equation, where T_A and T_B were determined to be respectively. -23,100 ±2000 and 244,000 ±20,000 cm^{-1}. It is assumed that the magnitudes of T_A and T_B 's were host independent within experimental error. (See Figure II)

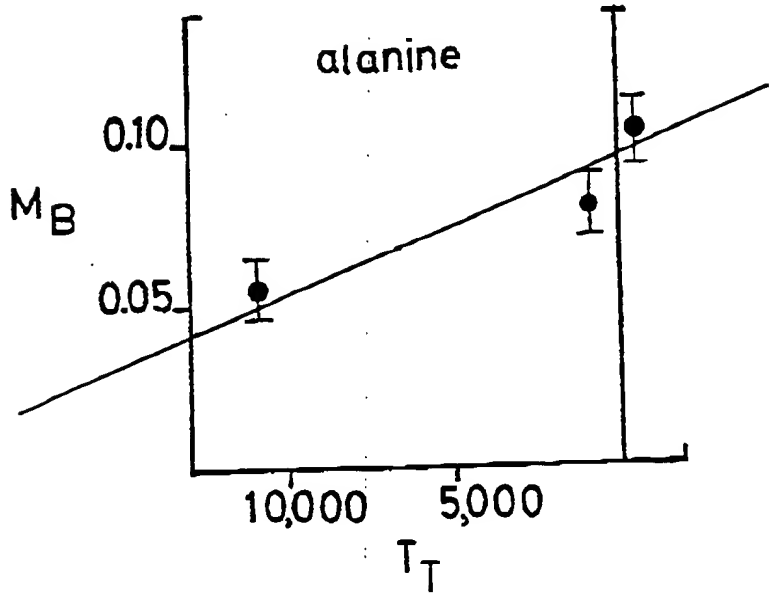

FIGURE II :- **The twisting powers for DEACl (alanine) derived for data shown in figure I are plotted as a function of M_B the mole fraction of isomer B calculated from ^{13}C NMR derived rotamer rotios @ 25 °C.**

The other chiral dopants DELCL (leucine), DEMCl (methionine), and DEMCCl (methyl cystiene) demonstrated the same general trends in the twisting power, ie host trimethyl - positive, host dimethyl - negative and host nomethyl - negative. For the chiral dopant DEMCCl no second rotamer was detected in the ^{13}C NMR spectra, and for the chiral dopants DELCl and DEMCl the rotamer ratio's were found to be .20 ±.04 and .21 ±.02 respectively, constant within experimental error. The rotamer ratios in these cases will be less important in determining the twisting power, but the nature of the head group now is much more important. T_A and T_B will now be a function of the host headgroup. The above three chiral dopants all have elongated sidechains in the chiral detergent headgroups, which will disrupt the chiral micelle surface.

With the chiral dopant DESCl (serine) there was no trend in the twisting powers the various host detergents, although the rotamer ratios are host dependent in a similar way to DEACl cases. Serine has an OH group in the side chain which will react strongly with the chiral micelle surface where T_A and T_B might be reversed. Although the molecular stereo chemistry of the chiral headgroup in all cases is similar the dissymmetry of the molecular polarization and hence the molecular chirality and bulk chirality in this case DESCl is more than likely reversed, as was observed with two of the hosts.

CONCLUSIONS

^{13}C NMR reveals that the decyl esters of four of the five amino acids investigated occurr as two rotamers. In the case of serine and alanine the rotamer ratio was host detergent dependent, but host detergent independent in the case of leucine and methionine. These two rotamers each make an opposite in sense and unequal in magnitude contribution to the total twisting power. These contributions in all cases except alanine appear to be host detergent dependent. There also may be evidence to suggest that the basic assumption that there is no inte-detergent interactions is not valid.

ACKNOWLEDGMENTS

Thanks to Professor M I Page in the Department of Chemical and Biological Sciences for providing research facilities. The University is thanked for providing a small research grant to buy chemicals.

REFERENCES

1. K. D. Lawson and T. J. Flaut, J.Am. Chem. Soc. **89**.5489 (1967)
2. K. Radley and A.Saupe, Mol. Phys. **35**. 1405 (1978)
3. K.Radley, G. J. Lilly, P. R. Patel, H. K. Cheema and Z. M. Rais, Mol. Cryst. Liq. Cryst. **268** 107. (1995)
4. W. E. Stewart and T. H. Siddall III, Chem. Rev. **5** 517 (1970)
5. M. Acimis and L. W. Reeves, Can. J. Chem. **58** 1533 (1980)
6. K. Radley and N. McLay, J. Phys. Chem. **98** 3071 (1994)
7. K. B. Wilberg and K. E. Laidig, J. Am. Chem. Soc. **109** 5935 (1987)
8. S. Ruschin and S. H. Bauer, J. Phys. Chem. **84** 3061 (1980)
9. A. P. Laws and M. I. Page, J. Chem. Soc. Perkins Trans II 1577 (1989)
10 C. Loubser, P. L. Wessels, P. Stryring and J. W. Goodby, J. Mater. Chem. **4** 71.(1994)

STIC-ILL

From: Schnizer, Richard
Sent: Tuesday, June 15, 2004 1:13 PM
To: STIC-ILL
Subject: 09/555,574

Please send me a copy of :

Radley et al (Molecular Crystals and Liquid Crystals Science and Technology, Section A: Molecular Crystals nad Liquid Crystals (1997), 303: 249-254

Ziady et al (Am. J. Physiol. (197) 273(2, part 1): G545-G552)

Legendre et al (Bioconj. Chem. (1997) 8(1): 57-63)

Wáshwa et al (Bioconjugate Chemistry (1997) 8(1): 81-88

Thank you-

Richard Schnizer, Ph.D.
Patent Examiner
Art Unit 1635
Remsen 2C01
571-272-0762
Mail Box 2C18

Peptide-Mediated Gene Delivery: Influence of Peptide Structure on Gene Expression

Manpreet S. Wadhwa,† Wendy T. Collard, Roger C. Adami, Donald L. McKenzie, and Kevin G. Rice*

Divisions of Medicinal Chemistry and Pharmaceutics, College of Pharmacy, University of Michigan, 428 Church Street, Ann Arbor, Michigan 48109. Received September 13, 1996®

Cationic peptides possessing a single cysteine, tryptophan, and lysine repeat were synthesized to define the minimal peptide length needed to mediate transient gene expression in mammalian cells. The N-terminal cysteine in each peptide was either alkylated or oxidatively dimerized to produce peptides possessing lysine chains of 3, 6, 8, 13, 16, 18, 26, and 36 residues. Each synthetic peptide was studied for its ability to condense plasmid DNA and compared to polylysine$_{19}$ and cationic lipids to establish relative *in vitro* gene transfer efficiency in HepG2 and COS 7 cells. Peptides with lysine repeats of 13 or more bound DNA tightly and produced condensates that decreased in mean diameter from 231 to 53 nm as lysine chain length increased. In contrast, peptides possessing 8 or fewer lysine residues were similar to polylysine$_{19}$, which bound DNA weakly and produced large (0.7–3 μm) DNA condensates. The luciferase expression was elevated 1000-fold after HepG2 cells were transfected with DNA condensates prepared with alkylated Cys-Trp-Lys$_{18}$ (AlkCWK$_{18}$) versus polylysine$_{19}$. The gene transfer efficiencies of AlkCWK$_{18}$ and cationic lipids were equivalent in HepG2 cells but different by 10-fold in COS 7 cells. A 40-fold reduction in particle size and a 1000-fold amplification in transfection efficiency for AlkCWK$_{18}$ DNA condensates relative to polylysine$_{19}$ DNA condensates suggest a contribution from tryptophan that leads to enhanced gene transfer properties for AlkCWK$_{18}$. Tryptophan-containing cationic peptides result in the formation of small DNA condensates that mediate efficient nonspecific gene transfer in mammalian cells. Due to their low toxicity, these peptides may find utility as carriers for nonspecific gene delivery or may be developed further as low molecular weight DNA condensing agents used in targeted gene delivery systems.

Nonviral gene delivery systems are being developed to transfect mammalian host cells with foreign genes (*1–3*). Plasmids encoding transgenes are complexed with carriers that facilitate the transfer of the DNA across the cell membrane for delivery to the nucleus. The efficiency of gene transfer into cells directly influences the resultant gene expression levels. Thereby, optimizing transfer efficiency is often necessary to achieve therapeutically relevant gene expression levels in a variety of host cells (*4, 5*).

Nonviral gene delivery systems rely on carrier molecules to bind and condense DNA into small particles that facilitate DNA entry into cells through endocytosis or pinocytosis (*1*). In addition, the carrier molecules act as scaffolding to which ligands may be attached to achieve site specific targeting of DNA (*6–15*).

The most commonly used DNA condensing agent for the development of nonviral gene delivery systems is polylysine in the size range of dp 90–450 (*6–15*). Its amino groups have been derivatized with asialoorosomucoid, transferrin, carbohydrates, folate, lectins, antibodies, or other proteins to provide specificity in cell recognition, without compromising its binding affinity for DNA (*6–15*). However, the high molecular weight and polydispersity of polylysine also contribute to a lack of chemical control in coupling macromolecular ligands, which leads to heterogeneity in polylysine-based carrier molecules. This can complicate the formulation of DNA carrier complexes and limits the ability to systematically optimize carrier design to achieve maximal efficiency (*16, 17*).

To refine targeted gene delivery carriers aimed at transfecting hepatocytes via the asialolglycoprotein receptor, we previously developed a low molecular weight carrier (4500) by attaching a single complex carbohydrate ligand to low molecular weight polylysine (dp 19) (*18*). This glycopeptide bound to DNA and efficiently transfected HepG2 cells *in vitro* via the asialolglycoprotein receptor, establishing that low molecular weight glycopeptide carriers can function as efficiently as a macromolecular glycoconjugate carriers. However, despite the low molecular weight of this glycopeptide, the polydispersity of polylysine$_{19}$ and the lack of control of the carbohydrate coupling site both contributed to heterogeneity, limiting further opportunity for optimization.

In the present study we have taken the next step toward developing homogeneous glycopeptide carriers by attempting to define the minimal polylysine chain length that leads to DNA condensation. Earlier studies examined the influence of polylysine chain length for transferrin–polylysine-mediated gene delivery and found that the transfection efficiency decreased below dp 300 (*12, 19*). Another study examined the particle size of DNA condensates produced with polylysine varying in size from dp 30 to 1500 and found that low molecular weight polylysine condensed DNA into small particles (20–30 nm) and was also less toxic to cells in culture (*20*). Still others have quantitatively examined the binding of lysine-rich peptides (dp 3–10) to single- and double-stranded oligonucleotides and noted an enhancement in the binding affinity when increasing polylysine chain length up to dp 10 (*21–23*). Notably, the peptides utilized in these studies contained a tryptophan residue that allowed monitoring of DNA binding via fluorescence.

* Author to whom correspondence should be addressed [telephone (313) 763-1032; fax (313) 763-2022; e-mail krice@umich.edu].

† Present address: GeneMedicine, Inc., 8301 New Trails Drive, The Woodlands, TX 77381-4248.

® Abstract published in *Advance ACS Abstracts,* December 15, 1996.

S1043-1802(96)00079-1 CCC: $14.00

A recent paper also highlighted the utility of a low molecular weight peptide (dp 13) possessing a lysine repeat of 8 as a DNA condensing for enhancing gene transfer (*24*). When coformulated with a fusogenic peptide and a plasmid encoding luciferase, this peptide mediated gene transfer in several cell lines, including hepatocytes, with efficiency comparable to that of cationic lipid mediated gene delivery.

The synthetic peptides used in the present study also possess a lysine repeat, which was varied from 3 to 36 residues and incorporated one or more tryptophan and cysteine residues. The results establish that a peptide of 13−18 lysine residues possessing a single tryptophan residue enhances gene transfer to cells in culture by up to 3 orders of magnitude relative to comparable polylysine peptides lacking a tryptophan. The mechanism of peptide-mediated gene transfer is related to the efficiency of condensing DNA into small particles. It is proposed that tryptophan plays a specific role in organizing the DNA binding of cationic peptides to produce small condensates that exhibit enhanced gene transfer efficiency. Therefore, tryptophan-containing peptides represent a new class of low molecular weight condensing agents that may be modified with ligands to produce low molecular weight carriers for site specific gene delivery.

MATERIALS AND METHODS

N-terminal Fmoc protected amino acids, and all other reagents for peptide synthesis, were obtained from Advanced ChemTech, Lexington, KY. Minimum essential media (MEM[1]), Sephadex G-25, dithiothreitol, iodoacetamide, iodoacetic acid, and polylysine$_{19}$ (MW 1000−4000) were purchased from Sigma Chemical Co., St. Louis, MO. Ethanedithiol (EDT) was purchased from Aldrich Chemical Co., Milwaukee, WI. Trifluoroacetic acid (TFA) was purchased from Fisher Scientific, Pittsburgh, PA. LB media, LB agar, D-luciferin, and luciferase from *Photinus pyralis* (EC 1.13.12.7) were obtained from Boehringer Mannheim, Indianapolis, IN. HepG2 and COS 7 cells were from the American Type Culture Collection, Rockville, MD. Dulbecco's modified Eagle medium (DMEM), media supplements, and heat inactivated "qualified" fetal bovine serum (FBS) were from Gibco BRL, Grand Island, NY. Bradford reagent was purchased from Bio-Rad, Hercules, CA, and thiazole orange was a gift from Beckton Dickinson Immunocytometry Systems, San Jose, CA. The 5.6 kb plasmid pCMVL encoding the reporter gene luciferase under the control of the cytomegalovirus promoter was a gift from Dr. M. A. Hickman at the University of California, Davis. Peptide purification was performed using a semipreparative (10 μm) C_{18} RP-HPLC column from Vydac, Hesperia, CA. HPLC was performed using a computer-interfaced HPLC and fraction collector from ISCO, Lincoln, NE.

DNA Purification and Peptide Synthesis. Plasmid DNA was prepared by the alkaline lysis method and purified on cesium chloride gradient (*25*). Peptides were prepared by solid phase peptide synthesis on Fmoc-L-Boc-lysine-Wang resin (*p*-benzyloxybenzyl alcohol resin, 1% divinyl benzene cross-linked, 100−200 mesh) at a 136 μmol scale (0.68 mmol/g resin). The synthesis was accomplished using a computer-interfaced Model 90 synthesizer from Advanced Chemtech. Lysine and tryptophan side chains were Boc protected, and the sulfhydryl side chain of cysteine was protected with a trityl group. A 6 molar excess of N-terminal Fmoc-protected amino acid was activated *in situ* in the reaction vessel by adding equimolar diisopropylcarbodiimide and *N*-hydroxybenzotriazole in a total reaction volume of 18 mL. Coupling was carried out for 1 h and was followed with a capping cycle for 30 min with 10% acetic anhydride in 1% diisopropylethylamine. Fmoc deblocking was performed with 25% piperidine for 12 min. All reagents were dissolved in dimethylformamide.

At completion, the resin-conjugated peptide was washed with dichloromethane, dried, and weighed. Cleavage was performed in a solution of TFA/EDT/water (95:2.5:2.5 v/v) for 30 min at room temperature, which simultaneously deprotected the amino acid side chains. The peptide solution was extracted with diethyl ether, concentrated by rotary evaporation, and freeze-dried. Lyophilized crude peptides were dissolved in degassed and nitrogen-purged 0.1% TFA. Peptides (3 μmol per injection) were purified on a semipreparative (2 × 25 cm) C_{18} RP-HPLC column eluted at 10 mL/min with 0.1% TFA and acetonitrile (5−20% over 40 min) while absorbance was monitored at 280 nm, 1.0 AUFS. Purified peptides were concentrated by rotary evaporation, lyophilized, and stored dry at −20 °C.

Lyophilized peptides (1 μmol) were dissolved in 1 mL of nitrogen-purged 50 mM Tris HCl (pH 7.5) and reduced by the addition of 250 μL of 100 mM dithiothreitol prepared in the same buffer by reacting at room temperature for 30 min. Alkylation was carried out by adding 25 mg of solid iodoacetamide or iodoacetic acid followed by reaction for 1 h at room temperature. The alkylated peptides were acidified to pH 2.0 with TFA and purified by RP-HPLC as described above. The yield of each purified peptide (approximately 25%) was determined from the absorbance of tryptophan (ϵ_{280nm} = 5600 M^{-1} cm^{-1}). The TFA salt of polylysine$_{19}$ was prepared by chromatographing the hydrobromide salt on RP-HPLC eluted with 0.1% TFA and acetonitrile while detecting 214 nm as described above. The concentration of polylysine$_{19}$ was established by fluorescamine analysis (*26*) using a calibrated standard of AlkCWK$_{18}$ as a reference.

Dimeric peptides were prepared by dissolving 1 μmol of each purified CWK$_n$ (n = 3, 8, 13, or 18) peptide in Tris HCl (pH 7.5) followed by reaction at 37 °C for 24 h. Each dimeric peptide was purified using RP-HPLC as described above and quantified by Abs$_{280nm}$ (ϵ = 11 200 M^{-1} cm^{-1}).

Peptides were characterized using MALDI-TOF-MS. The peptide (1 nmol) was reconstituted in 100 μL of 0.1% acetic acid, and 1 μL was applied to the target and analyzed using a Vestec-2000 Laser Tec Research laser desorption linear time of flight mass spectrometer using insulin as the internal standard. The instrument was operated with 23 kV ion accelerating voltage and 3 kV multiplier voltage using a 337 nm VSL-SS& ND nitrogen laser with a 3 ns pulse width.

Formulation of Peptide DNA Condensates. Peptide DNA condensates were prepared at a final DNA concentration of 20 μg/mL and at a peptide/DNA stoichiometry varying from 0.1 to 1.5 nmol of peptide/μg of DNA. The condensates were formed by adding peptide (2−30 nmol) prepared in 500 μL of isotonic Hepes-buffered mannitol (HBM, 0.27 M mannitol, 5 mM sodium Hepes, pH 7.5) to 20 μg of DNA in 500 μL of HBM while vortexing, followed by equilibration at room temperature for 30 min.

[1] Abbreviations: RP-HPLC, reversed phase high-performance liquid chromatography; CWK, cysteine−tryptophan−lysine; TFA, trifluoroacetic acid; EDT, ethanedithiol; MALDI-TOF-MS, matrix-assisted time of flight mass spectrometry; RLU, relative light units; DTT, dithiothreitol; FBS, fetal bovine serum; MEM, minimal essential media; DMEM, Dulbecco's modified Eagle media; HBM, Hepes-buffered mannitol; QELS, quasi-elastic light scattering.

Sedimentation of DNA condensates was evaluated by measuring the concentration of DNA in solution before and after centrifugation. After peptide DNA condensates were formed as as described above, a 50 μL aliquot (1 μg of DNA) was diluted in 1 mL of water and the $Abs_{260\ nm}$ was determined on a Beckman DU640 spectrophotometer. Following centrifugation at 13000*g* for 4 min at room temperature, an identical aliquot was diluted with 1 mL of water and the concentration of DNA remaining in solution was determined. The ratio of absorbances subtracted from unity and multiplied by 100 was defined as the percent sedimentation.

Peptide binding to DNA was monitored by a fluorescence titration assay (*18*). A 1 μg aliquot of the peptide DNA condensate prepared as described above was diluted to 1 mL in HBM containing 0.1 μM thiazole orange. The fluorescence of the intercalated dye was measured on an LS50B fluorometer (Perkin-Elmer, U.K.) in a microcuvette by exciting at 500 nm while monitoring emission at 530 nm, with the slits set at 15 and 20 nm and photomultiplier gain set to 700 V. DNA condensation was monitored by measuring total scattered light at 90° by setting both monochromators to 500 nm and decreasing slit widths to 2.5 nm. Fluorescence and scattered light intensity blanks were subtracted from all values before data analysis.

Transmission electron microscopy was preformed by immobilizing condensed DNA on carbon-coated copper grids (3 mm diameter, 400 mesh; Electron Microscopy Sciences, Fort Washington, PA). Grids were glow discharged, and 3 μL of peptide DNA condensate (20 μg/mL), prepared as described above, was placed on the grid for 5 min. The grids were blotted dry and then stained by floating for 1.5 min on each of three 100 μL drops of uranyl acetate (1%, in 95% ethanol) followed by rinsing with 0.4% detergent solution (PhotoFlo, Kodak) and drying. Electron microscopy was performed using a Philips EM-100 transmission electron microscope.

Particle size analysis was measured for peptide DNA condensates prepared at a DNA concentration of 20 μg/mL in HBM and at a stoichiometry of 0.8 or 1.0 ($DiCWK_3$) nmol of peptide/μg of DNA. Samples were analyzed using a Nicomp 370 Autodilute submicrometer particle sizer in the solid particle mode, and acquisition was continued until the fit error was <10. The mean diameter and population distribution were computed from the diffusion coefficient using functions supplied by the instrument.

***In Vitro* Gene Transfection.** HepG2 cells (2×10^6 cells) were plated on 6 × 35 mm wells and grown to 40–70% confluency in MEM supplemented with 10% FBS, penicillin, and streptomycin (10 000 units/mL), sodium pyruvate (100 mM), and L-glutamine (200 mM). Transfections were performed in MEM (2 mL/35 mm well) with 2% FBS, with or without 80 μM chloroquine. Peptide DNA condensates (10 μg of DNA in 0.5 mL of HBM) were added dropwise to triplicate wells. After 5 h of incubation at 37 °C, the medium was replaced with MEM supplemented with 10% FBS.

Luciferase expression was determined at 24 h with some modification of a published method (*27*). Cells were washed twice with ice-cold phosphate-buffered saline (calcium and magnesium free) and then treated with 0.5 mL of ice-cold lysis buffer (25 mM Tris chloride, pH 7.8, 1 mM EDTA, 8 mM magnesium chloride, 1% Triton X-100, 1 mM DTT) for 10 min. The cell lysate mixture was scraped, transferred to 1.5 mL microcentrifuge tubes, and centrifuged for 7 min at 13000*g* at 4 °C to pellet debris.

Lysis buffer (300 μL), sodium ATP (4 μL of a 180 mM solution, pH 7, 4 °C), and cell lysate (100 μL, 4 °C) were combined in a test tube, briefly mixed, and immediately placed in the luminometer. Luciferase relative light units (RLU) were recorded on a Lumat LB 9501 (Berthold Systems, Germany) with 10 s integration after automatic injection of 100 μL of 0.5 mM D-luciferin (prepared fresh in lysis buffer without DTT). The RLU were converted into femtomoles using a standard curve generated each day using luciferase dissolved in Tris acetate, pH 7.5, and stored at −20 °C. The standard curve was constructed by adding a known amount of the enzyme (0.01–100 fmol with specific activity of 2.5 nanounits/fmol) to 35 mm wells containing 40–70% confluent HepG2 or COS 7 cells. The cells were processed as described above, resulting in a standard curve with an average slope of 130 000 RLU/fmol of enzyme.

Protein concentrations were measured by Bradford assay using bovine serum albumin as a standard (*28*). The amount of luciferase recovered in each sample was normalized to milligrams of protein, and the mean and standard deviation obtained from each triplicate are reported.

COS 7 cells were plated at 72 000 cells per well and grown to 50% confluency in DMEM (Gibco BRL) supplemented with penicillin (10 000 units/mL), L-glutamine (200 mM), and 10% FBS for 24 h. The cells were transfected as described for HepG2 cells.

Lipofectace (Gibco BRL, 1:2.5 w/w dimethyl dioctadecylammonium bromide and dioleoylphosphatidylethanolamine) was used to mediate nonspecific gene transfection according to the manufacturer's instructions. The ratio of DNA to Lipofectace was optimized for both COS 7 and HepG2 cells. An optimal DNA/Lipofectace ratio was achieved by dissolving 10 μg of DNA in 100 μL of serum free media (SFM) followed by adding 60 μL of Lipofectace prepared in 140 μL of SFM. The Lipofectace DNA complex was then diluted with 1.7 mL of SFM and used to transfect HepG2 or COS 7 cells for 5 h followed by replacement of the transfecting media with supplemented 10% FBS. The cells were incubated for a total of 24 h, then harvested, and analyzed for luciferase as described above.

Dose response curves were prepared by varying the dose from 1 to 50 μg of DNA while keeping the peptide/DNA stoichiometry fixed at 0.6 nmol/μg of DNA and normalizing the volume to 0.5 mL. Alternatively, a dose response curve for Lipofectace was prepared by varying the DNA dose from 1 to 20 μg while keeping the stoichiometry of Lipofectace to DNA constant and normalizing the total volume of each dose to 2 mL with SFM.

RESULTS

Design of Peptides for Gene Delivery. Cationic peptides were designed to probe the minimal size needed to mediate efficient gene transfer in mammalian cells. The synthetic strategy involved comparison of four peptides with various lysine chain lengths in the range of 3–18 residues. During peptide synthesis, truncated peptides were capped by N-acetylation and a tryptophan residue was placed near the N terminus to provide a chromophore for identification of full-length sequences during purification. This residue allows quantitation of peptide concentration and is also intended for use in monitoring fluorescence to evaluate peptide binding to DNA as previously described (*21*). In addition, each peptide possessed an N-terminal cysteine residue as a potential ligand attachment site.

The four peptides were alkylated with iodoacetamide to provide $AlkCWK_n$ (where n = 3, 8, 13, or 18 residues)

Table 1. Peptides for Gene Delivery

name	sequence	mass (obsd/calcd[a])
$AlkCWK_3$	Alk-S-Cys-Trp-$(Lys)_3$	750.2/750.0
$AlkCWK_8$	Alk-S-Cys-Trp-$(Lys)_8$	1391.1/1390.9
$AlkCWK_{13}$	Alk-S-Cys-Trp-$(Lys)_{13}$	2031.1/2031.8
$AlkCWK_{18}$	Alk-S-Cys-Trp-$(Lys)_{18}$	2672.7/2672.5
$DiCWK_3$	$(Lys)_3$-Trp-Cys-S-S-Cys-Trp-$(Lys)_3$	1382.5/1382.8
$DiCWK_8$	$(Lys)_8$-Trp-Cys-S-S-Cys-Trp-$(Lys)_8$	2664.5/2665.2
$DiCWK_{13}$	$(Lys)_{13}$-Trp-Cys-S-S-Cys-Trp-$(Lys)_{13}$	3946.2/3945.9
$DiCWK_{18}$	$(Lys)_{18}$-Trp-Cys-S-S-Cys-Trp-$(Lys)_{18}$	5227.8/5227.9
$polylysine_{19}$	$(Lys)_{19}$	nd[b]/2435.8

[a] Masses are calculated as the average M + 1 of the free base. [b] The mass of $polylysine_{19}$ was not determined due to polydispersity.

(Table 1). A further extension of this peptide series was accomplished by allowing the cysteine of each monomeric peptide to oxidize, resulting in a panel of homodimeric peptides each possessing two tryptophans and a discontinuous lysine repeat of either 6, 16, 26, or 36 residues in length (Table 1). Each alkylated peptide and dimeric peptide was characterized using MALDI-TOF-MS, which produced a dominant ion corresponding to the anticipated molecular weight of each peptide (Table 1).

Purified $AlkCWK_3$, $AlkCWK_8$, $AlkCWK_{13}$, and $AlkCWK_{18}$ each demonstrated a minor (10%) peak eluting later than the major product on RP-HPLC. On storage in an acid solution, the minor peak increased proportionally to the loss of the major product. The new product was isolated and analyzed by MALDI-TOF-MS, which verified a loss of 17 amu. A byproduct of identical mass loss was formed for each of $AlkCWK_3$, $AlkCWK_8$, $AlkCWK_{13}$, and $AlkCWK_{18}$. We speculate that the new product represents a cyclization of N-terminal amine with the acetamido group attached to cysteine leading to the loss of ammonia. The proposed cyclic byproduct of $AlkCWK_{18}$ was isolated and found to be functionally equivalent to the parent structure in transfection assays. Substitution of iodoacetic acid for iodoacetamide in the alkylation step led to an $AlkCWK_{18}$ peptide that was acid stable and functionally equivalent in formulation and biological assays.

Peptide Binding to Plasmid DNA. Peptides were studied for DNA binding using a dye exclusion assay that has been described previously (*18*). Peptide binding to DNA leads to exclusion of thiazole orange intercalation and a decrease in fluorescence. Titration of $AlkCWK_3$, $AlkCWK_8$, $AlkCWK_{13}$, or $AlkCWK_{18}$ with DNA in the range of 0.1−1.5 nmol of peptide/μg of DNA led to a reduction in fluorescence except for the smallest peptide ($AlkCWK_3$), which failed to exclude the intercalator within the titration range (Figure 1A). An asymptote in the fluorescence decline was observed at a stoichiometry of 0.6, 0.4, or 0.2 nmol of peptide/μg of DNA for $AlkCWK_8$, $AlkCWK_{13}$, or $AlkCWK_{18}$, respectively (Figure 1A). The relative fluorescence intensity at peptide/DNA stoichiometries above the asymptote established that $AlkCWK_{13}$ and $AlkCWK_{18}$ were able to exclude thiazole orange intercalation more efficiently than $AlkCWK_8$.

Dimeric peptides ($DiCWK_n$, n = 8, 13, 18) also possessed high affinity for DNA as evidenced by the stoichiometry of the fluorescence asymptote and the reduction in residual fluorescence, both of which correlated with the number of lysine residues (Figure 1B). Of this series, $DiCWK_3$ possessed weak affinity for DNA and thereby produced an asymptote at a stoichiometry of 1 nmol of peptide/μg of DNA.

In contrast to these results, $polylysine_{19}$ demonstrated a markedly different fluorescence titration curve compared to the alkylated or dimeric peptides of comparable length (Figure 1C). Even though $polylysine_{19}$ has a similar number of lysine residues as $AlkCWK_{18}$, its fluorescence asymptote occurs at a stoichiometry of approximately 0.6 nmol of peptide/μg of DNA. This result suggests that $polylysine_{19}$ binding to DNA is weak relative to $AlkCWK_{18}$.

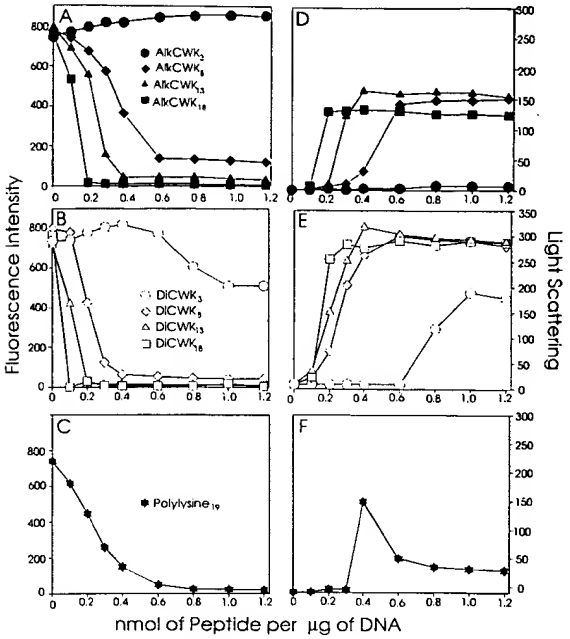

Figure 1. Fluorescence and light scattering titration of peptides with DNA. (A) Thiazole orange fluorescence was determined after titrating $AlkCWK_3$, $AlkCWK_8$, $AlkCWK_{13}$, or $AlkCWK_{18}$ with DNA as described under Materials and Methods. (D) Total light scattering measured simultaneously for each peptide DNA condensate. (B, E) Results of the fluorescence and light scattering titration using $DiCWK_3$, $DiCWK_8$, $DiCWK_{13}$, or $DiCWK_{18}$, respectively. (C, F) Fluorescence and light scattering titration of DNA with $polylysine_{19}$, respectively. Each titration represents the average of three determinations with average standard deviations of 7.4% for the fluorescence titration and 6.2% for the light scattering assay (error bars not shown).

Condensation of DNA with Peptides. Total light scattering at 90° was used to detect the peptide stoichiometry at which condensed DNA particles were formed (*18, 29*). Titration of $AlkCWK_8$, $AlkCWK_{13}$, or $AlkCWK_{18}$ with DNA produced a maximal total light scattering at stoichiometries that corresponded to the asymptote observed in the fluorescence exclusion assay (Figure 1D). A plateau in the light scattering profile observed at stoichiometries of 0.6, 0.4, and 0.2 for $AlkCWK_8$, $AlkCWK_{13}$, and $AlkCWK_{18}$, respectively, established the complete condensation of DNA at or above this peptide/DNA ratio. In contrast, titration of DNA with $AlkCWK_3$ failed to produce an increase in the light scattering, supporting earlier observations that indicate $AlkCWK_3$ fails to bind to DNA.

Titration of the dimeric peptides with DNA each produced condensates detected by light scattering (Figure 1E). Although the plateau light scattering levels for each dimeric peptide DNA condensate were nearly indistinguishable, the stoichiometry at which the plateau was achieved occurred at 0.6, 0.4, and 0.2 nmol of peptide/μg of DNA for $DiCWK_8$, $DiCWK_{13}$, and $DiCWK_{18}$, respectively. A weaker binding affinity for $DiCWK_3$ was evident from the plateau in light scattering which occurred at a stoichiometry of 1 nmol/μg of DNA (Figure 1E).

The light scattering profile for $polylysine_{19}$ was very distinct from that obtained for alkylated and dimeric

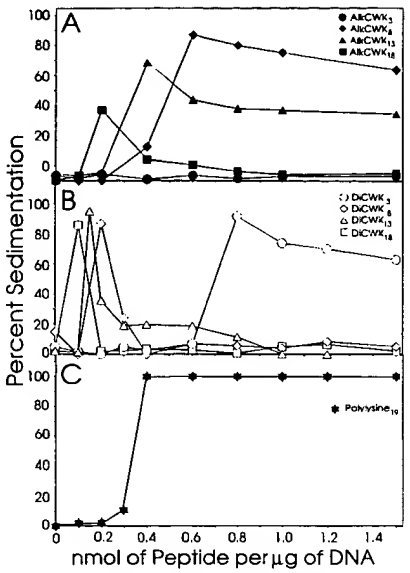

Figure 2. Sedimentation of peptide DNA condensates. The percent of DNA sedimented following centrifugation of peptide-induced DNA condensates is shown. The peptide/DNA stoichiometry was varied from 0.1 to 1.5 nmol of peptide/μg of DNA in HBM at a total DNA concentration of 20 μg/mL. (A) Results for $AlkCWK_3$, $AlkCWK_8$, $AlkCWK_{13}$, and $AlkCWK_{18}$; (B) results for $DiCWK_3$, $DiCWK_8$, $DiCWK_{13}$, and $DiCWK_{18}$; (C) results for $polylysine_{19}$. The average standard deviation for the assay was 8.6% (error bars not shown).

peptides. A sharp increase occurred at a stoichiometry of 0.4 nmol/μg of DNA, which declined to approximately 50 light scattering units at higher peptide/DNA stoichiometries (Figure 1F). This light scattering titration profile distinguished the condensation properties of $polylysine_{19}$ from CWK_n peptides, suggesting differences in the particle size for $polylysine_{19}$ DNA condensates.

Sedimentation of DNA Condensates. To evaluate the relative particle size of DNA condensates prepared at stoichiometries ranging from 0.1 to 1.5 nmol of peptide/μg of DNA, a sedimentation assay was utilized to measure the DNA remaining in suspension following centrifugation at 13000*g* for 4 min (*18*) (Figure 2). Titration of DNA with $AlkCWK_3$ resulted in the complete recovery of the DNA following centrifugation, supporting earlier findings that indicate $AlkCWK_3$ fails to bind and condense DNA into particles. Alternatively, $AlkCWK_8$, $AlkCWK_{13}$, and $AlkCWK_{18}$ each produced maximal sedimentation at a stoichiometry that roughly correlates with the stoichiometry calculated for a charge neutral complex (Figure 2A). At stoichiometries greater than charge neutral, $AlkCWK_8$ condensates sedimented to a greater extent than $AlkCWK_{13}$ or $AlkCWK_{18}$ condensates, indicating their larger size.

A similar trend was observed when dimeric peptide DNA condensates were sedimented. The maximal sedimentation was observed at a stoichiometry of 0.8, 0.2, 0.15, and 0.1 nmol of peptide/μg of DNA for $DiCWK_3$, $DiCWK_8$, $DiCWK_{13}$, and $DiCWK_{18}$, respectively (Figure 2B). At stoichiometries above the calculated charge neutral point $DiCWK_8$, $DiCWK_{13}$, and $DiCWK_{18}$ DNA condensates failed to sediment, suggesting they are smaller in size (Figure 2B). It is also evident that $DiCWK_3$ DNA condensates were large due to the observed sedimentation (70–80%) at stoichiometries above the charge neutralization point (Figure 2B).

In contrast, $polylysine_{19}$ DNA condensates sedimented completely at 0.2 nmol of peptide/μg of DNA and failed to recover at higher stoichiometries. These data established that once $polylysine_{19}$ DNA condensates are formed, they remained large throughout the titration range (Figure 2C).

Table 2. QELS Particle Size Distribution

peptide DNA condensate[a]	particle size population diameter[b] (nm)	σ[c] (nm)
$polylysine_{19}$	3102	297
$AlkCWK_3$		
$AlkCWK_8$	2412	354
$AlkCWK_{13}$	231	107
$AlkCWK_{18}$	78	30
$DiCWK_3$	724	154
$DiCWK_8$	53	24
$DiCWK_{13}$	56	29
$DiCWK_{18}$	64	27

[a] Peptide DNA condensates were prepared at a concentration of 20 μg/mL of DNA and at stoichiometry of 0.8 or 1.0 nmol ($DiCWK_3$) of peptide/μg of DNA in HBM. [b] Represents the mean diameter of particles. [c] Standard deviation of the population.

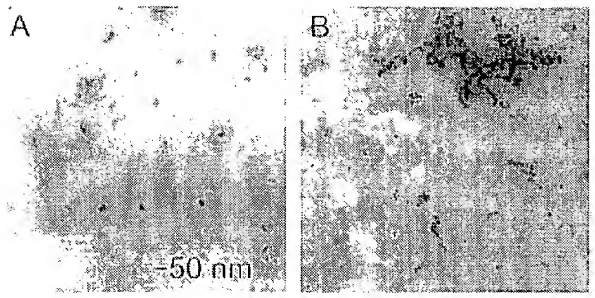

Figure 3. Electron microscopy of DNA condensates. The electron micrographs are shown for DNA condensates prepared at 0.5 nmol of peptide/μg of DNA for $AlkCWK_{18}$ (A) and at 0.8 nmol of peptide/μg of DNA for $polylysine_{19}$ (B). The calibration bar shown is 50 nm in length.

Particle Size and Distribution. DNA condensates were prepared with alkylated peptides, dimeric peptides, and $polylysine_{19}$ at a stoichiometry of 0.8 nmol of peptide/μg of DNA, and particle sizes were compared using quasi-elastic light scattering (QELS). A population of particles with average diameters of 0.7–3.1 μm was determined for $polylysine_{19}$, $AlkCWK_8$, and $DiCWK_3$ DNA condensates, whereas no particles were detected for $AlkCWK_3$ DNA condensates (Table 2), consistent with the results of sedimentation analysis.

Each alkylated or dimeric peptide possessing 13 lysine residues or more produced a population of particles with mean diameters of 53–231 nm (Table 2). It should be noted that particle populations were most often bimodal, possessing a major (>90%) smaller diameter population and a minor larger diameter population which contributed to the large standard deviation of the average particle size (Table 2).

Particle sizes determined by QELS were substantiated by analyzing DNA condensates using electron microscopy. Figure 3 compares the particle size and morphology for $AlkCWK_{18}$ and $polylysine_{19}$ DNA condensates. The images demonstrate that condensates produced with $AlkCWK_{18}$ are relatively uniform particles with diameters of approximately 50–100 nm, whereas $polylysine_{19}$-induced condensates were large flocculated particles, consistent with the result of particle size analysis by QELS (Figure 3).

***In Vitro* Gene Expression of Peptide DNA Condensates.** Luciferase reporter gene expression was analyzed following transfection of HepG2 or COS 7 cells with peptide DNA condensates prepared at stoichiometries ranging from 0.1 to 1.5 nmol of peptide/μg of DNA.

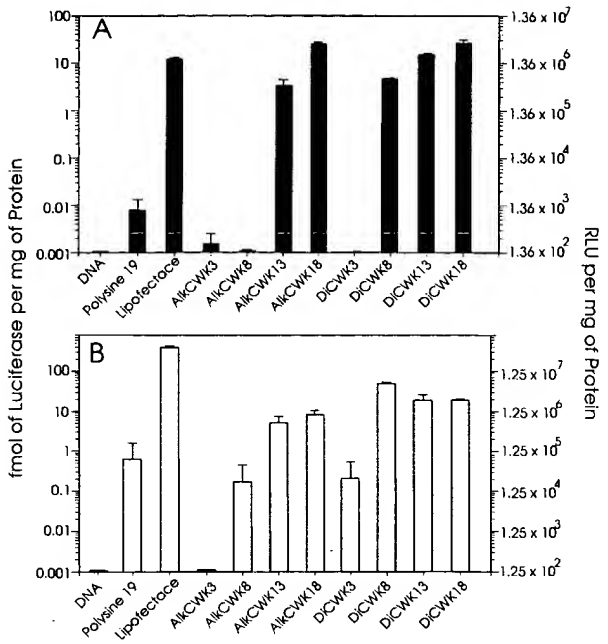

Figure 4. In vitro gene expression in HepG2 and COS 7 cells. Luciferase reporter gene expression is shown for DNA condensates prepared using alkylated peptides, dimeric peptides, polylysine$_{19}$, and Lipofectace. Chloroquine (80 μM) was included in the transfecting media for peptides and polylysine$_{19}$. (A) Gene expression determined in HepG2 cells; (B) gene expression in COS 7 cells. Each bar represents the mean and standard deviation of three determinations.

A 10-fold enhancement in the gene expression level was achieved when chloroquine was included in the transfecting media. For each peptide-condensing agent, the maximal reporter gene expression occurred at a peptide/DNA stoichiometry that corresponds to the fully condensed DNA as determined by the asymptote in the light scattering assay (Figure 1D,E,F) (*18*). At stoichiometries greater than that required to achieve condensation, the gene expression remained constant. Thereby, the relative gene expression levels were compared for each peptide DNA condensate at a fixed stoichiometry of 0.8 or 1.0 nmol (DiCWK$_3$) of peptide/μg of DNA, which was sufficient for each peptide to fully condense DNA.

Transfection of HepG2 with 10 μg of either uncomplexed plasmid DNA, AlkCWK$_3$ or AlkCWK$_8$, DiCWK$_3$, or polylysine$_{19}$ DNA condensates failed to produce significant reporter gene expression (Figure 4A). This result supported formulation experiments that predicted these peptides either fail to condense DNA (AlkCWK$_3$) or produce condensates that are large (0.7−3.1 μm). Alternatively, AlkCWK$_{13}$, AlkCWK$_{18}$, DiCWK$_8$, DiCWK$_{13}$, and DiCWK$_{18}$ DNA condensates each demonstrated significant gene transfer efficiency that was 2−3 orders of magnitude greater than that of polylysine$_{19}$. Lipofectace-mediated gene expression levels were also found to be identical to peptide-mediated expression levels in HepG2 cells (Figure 4A).

To verify that peptide-mediated gene delivery was not dependent on the existence of cell type specific receptors, the reporter gene expression in HepG2 cells was compared to that in COS 7 cells (Figure 4B). Significant differences were observed for the transfection of COS 7 versus HepG2 cells such that only uncomplexed DNA and AlkCWK$_3$ DNA condensates failed to produce measurable gene expression levels. AlkCWK$_8$, DiCWK$_3$, and polylysine$_{19}$ DNA condensates each mediated a significant gene expression in COS 7 cells despite their inactivity

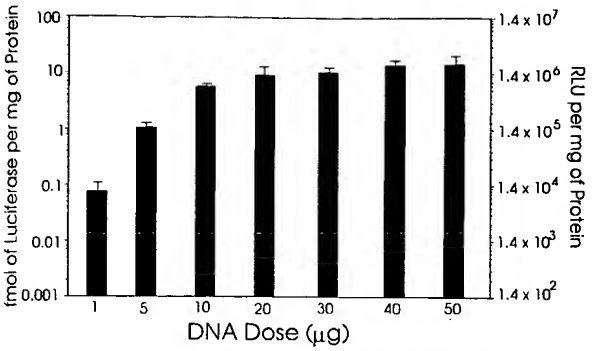

Figure 5. Dose response for peptide-mediated gene delivery. Luciferase gene expression levels in HepG2 are compared using an escalating dose of AlkCWK$_{18}$ DNA condensate prepared at a stoichiometry of 0.6 nmol/μg of DNA.

in transfecting HepG2 cells. However, the gene expression level mediated by these peptides was still 1−2 orders of magnitude below that afforded by AlkCWK$_{13}$, AlkCWK$_{18}$, DiCWK$_8$, DiCWK$_{13}$, and DiCWK$_{18}$ (Figure 4B). Also, Lipofectace-mediated gene expression in COS 7 cells was 1 order of magnitude greater than peptide-mediated gene delivery. These results suggest that the size restriction of peptide DNA condensates is less stringent in COS 7 cells compared to HepG2 cells.

To establish the effect of dose response using peptide DNA condensates, HepG2 cells were treated with escalating doses of AlkCWK$_{18}$ DNA condensates and Lipofectace DNA formulations. As demonstrated in Figure 5, a dose response curve for the AlkCWK$_{18}$ DNA condensate plateaus at 20 μg of DNA and remains constant at higher doses, whereas the toxicity of Lipofectace above 10 μg of DNA (data not shown) leads to reduced expression levels at higher doses.

DISCUSSION

The efficiency of carrier-mediated gene delivery depends on the reversible association of condensing molecules with plasmid DNA (*1*−*3*). The carriers that have been used most often are composed of polymers or lipids that bind to anionic sites on DNA. In the case of cationic peptides, this leads to condensation of plasmid DNA into small particles that gain entry into the target cell via nonspecific fluid phase pinocytosis (*1*). Attachment of ligands adds specificity to the delivery system and likewise alters the mode of DNA transfer across cell membranes such that DNA and ligand cotransfer via receptor-mediated endocytosis (*5*−*15*).

Previously we demonstrated that a low molecular weight glycopeptide mediated gene transfer to hepatocytes via the asialoglycoprotein receptor (*18*). Since this glycopeptide was prepared from low molecular weight polydisperse polylysine (dp 19), we sought to systematically optimize the peptide portion of the glycopeptide as a first step to improve its efficiency as a carrier for nonviral gene delivery.

The results establish that low molecular weight peptides possessing six or more lysine residues bind with sufficient affinity to condense DNA at stoichiometries above the charge neutral point (Figure 1). However, condensation of DNA is not sufficient to ensure significant transfection levels since AlkCWK$_8$, DiCWK$_3$, and polylysine$_{19}$ each produced DNA condensates but failed to mediate significant gene transfer in HepG2 cells (Figure 4A). The success or failure of individual peptide DNA condensates to mediate gene expression appears to be related to particle size such that larger condensates

are less efficiently pinocytosed (*2*). For HepG2 cells an apparent size restriction exists that excludes large DNA condensates. This is demonstrated by comparison of the transfection efficiency for $AlkCWK_8$ DNA condensates of 2.4 μm size relative to $AlkCWK_{13}$ DNA condensates, which possess an average diameter of 231 nm (Figure 4A). The addition of five lysine residues decreases particle size 10-fold, which leads to a 1000-fold amplification in gene transfer efficiency. Further reductions in the DNA particle diameters in the range of 231−53 nm only led to an additional 10-fold increase in transfection levels (Figure 4A). The size requirements described above for transfecting HepG2 cells are less stringent for COS 7 cells. Large (0.7−3.1 μm) peptide DNA condensates are moderately efficient at mediating transfection in COS 7 cells but are still 10−100-fold less efficient than smaller DNA condensates (Figure 4B).

The equivalent transfer efficiency of peptide DNA condensates into either HepG2 or COS 7 cells suggests a nonspecific mechanism related to the cationic nature of the condensates (*1*, *2*). We have also transfected 293T cells with peptide DNA condensates (data not shown), which resulted in a similar high level of gene expression. Comparable gene expression levels were obtained using peptide or Lipofectace to mediate DNA transfer in HepG2 cells, whereas Lipofectace-mediated gene delivery was found to be more efficient that peptide-mediated gene delivery in COS 7 cells (Figure 4). These results reflect cell type specific differences that must be considered in the development of gene delivery systems (*1*, *2*).

The discovery of a class of low molecular weight peptides that efficiently condense DNA into small particles is a major finding of this study. Apparently, some structural feature of $AlkCWK_n$ peptides allows more efficient condensation of DNA relative to polylysine. This is demonstrated most clearly by $AlkCWK_{18}$, which condenses DNA into particles that are 40-fold smaller (78 nm) than those produced by $polylysine_{19}$ (3.1 μm). Given that the lysine chain lengths of these two peptides are nearly equivalent, the N-terminal cysteine or tryptophan is presumably responsible for the enhanced condensing activity. To investigate the structural requirements of an efficient DNA condensing peptide, we synthesized an isomer of $AlkCWK_{18}$ also possessing 18 lysine residues but in which cysteine is relocated to the C terminus and tryptophan is the N terminus ($WK_{18}C$). The alkylated and dimeric form of this peptide each mediated gene transfer as efficiently as $AlkCWK_{18}$ (data not shown), suggesting that the location of cysteine may not be key to the reported activity. On the basis of this and other observations discussed below, we hypothesize that tryptophan may be primarily responsible for the enhanced condensation activity of $AlkCWK_{18}$ compared to $polylysine_{19}$.

A tryptophan residue may increase the binding affinity between cationic peptides and DNA. Evidence supporting this hypothesis comes from the stoichiometry of $AlkCWK_{18}$ (0.2 nmol of peptide/μg of DNA) needed to exclude intercalator binding to DNA versus that for $polylysine_{19}$ (0.6 nmol of peptide/μg of DNA) (Figure 1A,C). Lohman and co-workers also identified a function for tryptophan in altering cationic peptide binding to DNA and RNA (*22*, *23*). Curiously, they determined an enhancement in the entropy of peptide binding to DNA when substituting tryptophan for lysine (*22*, *23*). However, this was offset by a decrease in the enthalpy of binding, leading to a net zero change in the association constant (*22*, *23*). These studies also established that the location of tryptophan is not important and that multiple tryptophan residues do not influence the magnitude of the association constant despite changes in the enthalpic and entropic contributions (*22*, *23*). Recently, a low molecular weight cationic peptide possessing alanine, tyrosine, 10 lysines, and tryptophan has been co-complexed with a fusogenic peptide and DNA to achieve a 5 order of magnitude amplification in gene expression in HepG2 cells relative to uncomplexed DNA (*24*). The efficient DNA condensing activity of this low molecular weight peptide may also be linked the tryptophan residue, which flanks the polylysine sequence.

The precise mechanism of how tryptophan functions to increase binding affinity and decrease particle size is uncertain; however, it may relate to its ability to intercalate into DNA leading to an observed fluorescence quench (*21*−*23*). Tryptophan's hydrophobic interaction with DNA may organize the peptide binding on DNA, facilitating the formation of intermolecular ion pairs between multiple lysine residues and the DNA phosphate backbone.

Preparation of small DNA condensates has also recently been reported using polylysine dp 30 at a stoichiometric excess of 1.2 nmol/μg of DNA (*20*). The present study establishes that simple amino acid substitutions allow polylysine peptides as small as dp 13 to acquire the necessary affinity to condense DNA into small particles at low stoichiometric excess.

The development of homogeneous peptides that actively condense DNA into small particles is an important advance toward the development of low molecular weight carriers for targeted gene delivery. Attachment of a receptor ligand such as a carbohydrate or peptide to a single cysteine residue should endow specificity to the gene delivery system and allow further systematic optimization of low molecular weight carriers for receptor-mediated gene delivery.

ACKNOWLEDGMENT

We acknowledge financial support for this work from NIH GM48049. The DNA used for these studies was prepared by Anna Calcagno. We also acknowledge technical assistance in performing mass spectroscopy by Bao-Jen Shyong at the Carbohydrate and Protein core facility, University of Michigan. Electron microscopy studies were performed with technical assistance from Bruce Donohoe and Chris Edwards in the Department of Cell Biology and Anatomy, University of Michigan. The QELS particle size analysis was performed with assistance from Ramachandran Chandrasekharan at the College of Pharmacy, University of Michigan.

LITERATURE CITED

(1) Behr, J. P. (1994) Gene Transfer with Synthetic Cationic Amphiphiles: Prospects for Gene Therapy. *Bioconjugate Chem. 5*, 382−389.
(2) Ledley, F. D. (1995) Nonviral Gene Therapy: The Promise of Genes as Pharmaceuticals. *Hum. Gene Ther. 6*, 1129−1144.
(3) Christiano, R. J., and Roth, J. A. (1995) Molecular Conjugates: a Targeted Gene Delivery Vector For Molecular Medicine. *J. Mol. Med. 73*, 479−486.
(4) Ledley, T. S., and Ledley, F. D. (1994) Multicompartment, Numerical Model of Cellular Events in the Pharmacokinetics of Gene Therapies. *Hum. Gene Ther. 5*, 679−691.
(5) Michael, S. I., and Curiel, D. T. (1994) Strategies to Achieve Targeted Gene Delivery Via the Receptor-Mediated Endocytosis Pathway. *Gene Ther. 1*, 223−232.
(6) Wu, G. Y., and Wu, C. H. (1988) Evidence for Targeted Gene Delivery to HepG2 Hepatoma Cells in Vitro. *Biochemistry 27*, 887−892.
(7) Wu, G. Y., and Wu, C. Y. (1988) Receptor-Mediated Gene Delivery and Expression in Vivo. *J. Biol. Chem. 29*, 14621−14624.

(8) Huckett, B., Ariatti, M., and Hawtrey, A. O. (1990) Evidence for Targeted Gene Transfer by Receptor-Mediated Endocytosis. Stable Expression Following Insulin-Directed Entry of Neo Into HepG2 Cells. *Biochem. Pharmacol. 40*, 253−263.

(9) Thurnher, M., Wagner, E., Clausen, H., Mechtler, K., Rusconi, S., Dinter, A., Birnstiel, M. L., Berger, E. G., and Cotten, M. (1994) Carbohydrate Receptor-Mediated Gene Transfer to Human T-Leukaemic Cells. *Glycobiology 4*, 429−435.

(10) Rojanasakul, Y., Wang, L. Y., Malanga, C. J., Ma, J. K. H., and Liaw J. (1994) Targeted Gene Delivery to Alveolar Macrophages via Fc Receptor-Mediated Endocytosis. *Pharm. Res. 11*, 1731−1736.

(11) Midoux, P., Mendes, C., Legrand, A., Raimond, J., Mayer, R., Monsigny, M., and Roche, C. (1993) Specific Gene Transfer Meidated by Lactosylated Poly(L-Lysine) into Hepatoma Cells. *Nucleic Acid Res. 21*, 871−878.

(12) Wagner, E., Zenke, M., Cotten, M., Beug, H., and Birnstiel, M. L. (1990) Transferrin-Polycation conjugates as Carriers for DNA Uptake into Cells. *Proc. Natl. Acad. Sci. U.S.A. 87*, 3410−3414.

(13) Merwin, J. R., Noell, G. S., Thomas, W. L., Chiou, H. C., DeRome, M. E., McKee, T. D., Spitalny, G. L., and Findeis, M. A. (1994) Targeted Dlivery of DNA using YEE (GalNAcAH)3, a Synthetic Glycopeptide Ligand for the Asialoglycoprotein Receptor. *Bioconjugate Chem. 5*, 612−620.

(14) Yin, W., and Cheng, P. W. (1994) Lectin Conjugate-Directed Gene Transfer to Airway Epithelial Cells. *Biochem. Biophys. Res. Commun. 205*, 826−833.

(15) Gottschalk, S., Cristiano, R. J., Smith, L. C., and Woo, S. L. C. (1994) Folate Receptor Mediated DNA Delivery into Tumor Cells: Potosomal Disruption Results in Enhanced Gene Expression. *Gene Ther. 1*, 185−191.

(16) McKee, T. D., DeRome, M. E., Wu, G. Y., and Findeis, M. A. (1994) Preparation of Asailoorosomucoid-Polylysine Conjugates. *Bioconjugate Chem. 5*, 306−311.

(17) Erbacher, P., Roche, A. C., Monsigny, M., and Midoux, P. (1995) Glycosylated Polylysine/DNA Complexes: Gene Transfer Efficiency in Relation with the Size and Sugar Substitution Level of Glycosylated Polylysines and with the Plasmid Size. *Bioconjugate Chem. 6*, 401−410.

(18) Wadhwa, M., Knoell, D. L., Young, A. P., and Rice, K. G. (1995) Targeted Gene Delivery with A Low Molecular Weight Glycopeptide. *Bioconjugate Chem. 6*, 283−291.

(19) Taxman, D. J., Lee, E. S., and Wojchowski, D. M. (1993) Receptor-Targeted Transfection Using Stable Maleimido Transferrin/Thio-Polyl(L-Lysine) Conjugates. *Anal. Biochem. 213*, 97−103.

(20) Wolfert, M. A., and Seymour, L. W. (1996) Atomic Force Microscopic Analysis of the Influence of the Molecular Weight of Poly(L-Lysine) on the Size of Polyelectolyte Complexes Formed with DNA. *Gene Ther. 3*, 269−273.

(21) Bujalowski, W., and Lohman, T. M. (1987) A General Method of Analysis of Ligand-Macromolecule Equilibria Using a Spectroscopic Signal from the Ligand To Monitor Bining. Application to *Escherichia coli* Single-Strand Bining Protein-Nucleic Acid Interactions. *Biochemistry 26*, 3099−3106.

(22) Mascotti, D. P., and Lohman, T. M. (1992) Cooperative Binding of Polyamines Induces the *Escherichia coli* Single-Strand Binding Protein-DNA Binding Mode Transitions. *Biochemistry 31*, 8932−8946.

(23) Mascotti, D. P., and Lohman, T. M. (1993) Thermodynamics of Single-Stranded RNA and DNA Interactions with Oligolysines Containing Tryptophan. Effects of Base Composition. *Biochemistry 32*, 10568−10579.

(24) Gottschalk, S., Sparrow, J. T., Hauer, J., Mims, M. P., Leland, F. E., Woo, S. L. C., and Smith, L. C. (1996) A Novel DNA-Peptide Complex for Efficient Gene Transfer and Expression in Mammalian Cells. *Gene Ther. 3*, 448−457.

(25) Sambrook, J., Fritsch, E. F., and Maniatis, T. (1989) *Molecular Cloning: A Laboratory Manual*, Cold Spring Harbor Laboratory Press, Plainview, NY.

(26) Naoi, M., and Lee, Y. C. (1974) A Fluorometric Measurement of Ligands Incorporated into BrCn-Activated Polysaccharides. *Anal. Biochem. 57*, 640−644.

(27) Brasier, A. R., Tate, J. E., and Harener, J. F. (1989) Optimized Use of the Firefly Luciferase Assay as a Reproter Gene in Mammalian Cell Lines. *BioTechniques 7*, 1116−1122.

(28) Bradford, M. M. (1976) A Rapid and Sensitive Method for the Quantitation of Microgram Quantities of Protein Utilizing the Principle of Protein-Dye Binding. *Anal. Biochem. 72*, 248−254.

(29) Wilson, R. W., and Bloomfield, V. A. (1979) Counterion-induced Condensation of Deoxyribomucleic Acid. A Light Scattering Study. *Biochemistry 18*, 2192−2196.

BC960079Q

STIC-ILL

QP1.A5
MIC

From: Schnizer, Richard
Sent: Tuesday, June 15, 2004 1:13 PM
To: STIC-ILL
Subject: 09/555,574

Please send me a copy of :

Radley et al (Molecular Crystals and Liquid Crystals Science and Technology, Section A: Molecular Crystals nad Liquid Crystals (1997), 303: 249-254

Ziady et al (Am. J. Physiol. (197) 273(2, part 1): G545-G552)

Legendre et al (Bioconj. Chem. (1997) 8(1): 57-63)

Washwa et al (Bioconjugate Chemistry (1997) 8(1): 81-88

Thank you-

Richard Schnizer, Ph.D.
Patent Examiner
Art Unit 1635
Remsen 2C01
571-272-0762
Mail Box 2C18

Gene transfer into hepatoma cell lines via the serpin enzyme complex receptor

ASSEM-GALAL ZIADY,[1] JOSE C. PERALES,[2,3] THOMAS FERKOL,[3,4] THOMAS GERKEN,[2] HELGA BEEGEN,[2] DAVID H. PERLMUTTER,[5] AND PAMELA B. DAVIS[3]

Departments of [1]Physiology and Biophysics, [4]Pediatrics, and [2]Biochemistry, Case Western Reserve University School of Medicine, and [3]Copernicus Gene Systems, Cleveland, Ohio 44106; and [5]Department of Pediatrics, Cell Biology, and Physiology, Washington University School of Medicine, Saint Louis, Missouri 63110

Ziady, Assem-Galal, Jose C. Perales, Thomas Ferkol, Thomas Gerken, Helga Beegen, David H. Perlmutter, and Pamela B. Davis. Gene transfer into hepatoma cell lines via the serpin enzyme complex receptor. *Am. J. Physiol.* 273 (*Gastrointest. Liver Physiol.* 36): G545–G552, 1997.—The serpin enzyme complex receptor (SECR) expressed on hepatocytes binds to a conserved sequence in α_1-antitrypsin (α_1-AT) and other serpins. A molecular conjugate consisting of a synthetic peptide (C1315) based on the SECR binding motif of human α_1-AT covalently coupled to poly-L-lysine was used to introduce reporter genes into hepatoma cell lines in culture. This conjugate condensed DNA into spheroidal particles 18–25 nm in diameter. When transfected with the SECR-directed complex containing pGL3, Hep G2 cells that express the receptor, but not Hep G2 cells that do not, expressed a peak luciferase activity of 538,731 ± 144,346 integrated light units/mg protein 4 days after transfection. Free peptide inhibited uptake and expression in a dose-dependent manner. Complexes of DNA condensed with polylysine or LC-sulfo-*N*-succinimidyl-3-(2-pyridyldithio)propionate-substituted polylysine were ineffective. Transfection with a plasmid encoding human factor IX produced expression in Hep G2 (high) and HuH7 cells that express SECR but not Hep G2 (low) cells that lack the receptor. Fluorescein-labeled C1315 peptide labeled 9–31% of Hep G2 (high), 10–14% of HuH7, and 0.6–3.4% of Hep G2 (low) cells, and when the *lac* Z gene was transfected, only these cells expressed β-galactosidase. SECR-mediated gene transfer gives efficient, specific uptake and high-level expression of three reporter genes, and the system merits further study for gene therapy.

receptor-mediated gene transfer; liver cells; synthetic peptides; gene therapy

A NUMBER OF GENE TRANSFER systems have been developed in the search for efficient, yet safe, vectors for gene therapy (23). Replication-deficient recombinant viral vectors, as well as liposomes, have been used to deliver genes to a variety of cells (7, 10, 11, 29). However, despite their ability to accomplish gene delivery, these vectors are limited by practical and theoretical constraints (5, 7, 10, 23, 24). A less cytotoxic, more specific alternative to these gene transfer systems is gene delivery via the receptor-mediated endocytosis pathway (25, 30–32). For this approach, a carrier consisting of poly-L-lysine chemically conjugated to a receptor-specific ligand is noncovalently bound to expression plasmids. With careful manipulation of the ionic strength, DNA is condensed into complexes ranging in size from 10 to 25 nm in diameter (8, 9). Cotten et al. (6) reported delivery and expression of genes contained in 48-kilobase (kb) plasmids, demonstrating efficiency of this method in the transfer of large DNA (6). Thus the system affords tissue target specificity and is noninfectious. Furthermore, because receptor-mediated internalization is a ubiquitous physiological process, this form of gene therapy could be applied to a variety of cell types.

Since the initial reports by Wu and Wu (32) of receptor-mediated gene delivery to cells (32), a number of groups have demonstrated efficient gene transfer through targeting the transferrin (30, 31), asialoglycoprotein (25), polymeric immunoglobulin (8), and mannose (9) receptors in vitro and in vivo. These receptors have in common the ability to internalize large molecules in large quantities and, other than the binding motif of the ligand, have relaxed structural requirements for the remainder of the molecule.

The serine protease inhibitor (serpin) enzyme complex receptor (SECR) was originally described as a cell surface binding site on human hepatoma Hep G2 cells and blood monocytes. It recognizes a sequence on the carboxy-terminal tail of α_1-antitrypsin (α_1-AT) (27). A synthetic peptide (peptide 105Y) based in sequence on amino acids 359–374 of α_1-AT bound to Hep G2 cells in a manner both specific and saturable (13, 16, 18, 27, 28). Scatchard analysis estimated a dissociation constant (K_d) of ~40 nM and ~405,000 plasma membrane receptors per cell. The binding site defined in these early studies has been shown to bind α_1-AT itself but only when it is complexed with a serine protease, such as neutrophil elastase, or modified by either metalloelastase or by the collaborative action of active oxygen intermediates and neutrophil elastase (16, 27). Subsequent studies have shown that SECR mediates internalization of its ligands and delivers them to an acidic compartment, either late endosome or lysosome, for degradation (2, 28). It is now known to be expressed on a number of cell types, including mononuclear phagocytes, neutrophils, myeloid cell lines U937 and HL60, human intestinal epithelial cell line Caco-2, mouse fibroblast L cells, rat neuronal cell line PC12, and human glial cell line U373MG (2, 14, 26). On hepatoma cells SECR mediates feedback upregulation of endogenous α_1-AT synthesis (27). On neutrophils (14) it mediates the known chemotactic effect of α_1-AT-elastase complexes (1).

The SECR binding domain in the carboxy-terminal tail of α_1-AT is highly conserved among the serpin family, and, indeed, a number of SECs compete for binding to SECR (16, 27). Compatible sequences are also found in some tachykinins, including substance P and substance K, amyloid-β peptide, and bombesin (14,

15). Thus, similar to other receptors favorable for gene transfer, it is adapted for binding and internalizing large molecular complexes with relatively low selectivity as long as a pentapeptide binding domain FV(F/Y)L(I/M) is present (13, 15, 16, 18, 26, 27).

Exogenous DNA complexes bearing the pentapeptide binding motif could be targeted to and internalized by the SECR. Its abundance and bulk flow characteristics coupled to the prospect of targeting hepatocytes (the site of many recessive inherited disorders such as α_1-AT deficiency) as well as cells primarily affected by Alzheimer's disease (reviewed in Ref. 26), make this receptor system an attractive candidate for receptor-mediated gene delivery. Furthermore, its presence in the brain may provide the potential to transfer therapeutic genes across the blood-brain barrier. In this study we tested the hypothesis that foreign DNA condensed by poly-L-lysine coupled to a synthetic peptide ligand for the SECR (13, 18) can be targeted to and expressed in cells bearing the receptor in vitro.

MATERIALS AND METHODS

Materials. DNA-modifying enzymes, nucleotides, and 5-bromo-4 chloro-3-indolyl-β-D-galactopyranoside (X-gal) were purchased from Boehringer Mannheim (Indianapolis, IN). Poly-L-lysine was obtained from Sigma Chemical (St. Louis, MO) and LC-sulfo-*N*-succinimidyl-3-(2-pyridyldithio)propionate (LC-sulfo-SPDP) was purchased from Pierce Chemical (Rockford, IL). Luciferase activity was measured with the use of Promega (Madison, WI) assay reagents. Sephadex G_{10} columns and Bradford protein assay reagents were obtained from Bio-Rad (Richmond, CA). ^{125}I used for iodination was purchased from DuPont-New England Nuclear (Boston, MA). Peptide C105Y (CSIPPeVKFNKPFVYLI), and C1315 (CFLEAIPMSIPPEVKFNKPFVFLIIHRD) were synthesized by solid-phase method, purified, and subjected to amino acid composition and sequence analysis as described previously (13).

Cell culture. Two populations of human hepatoma Hep G2 cells were maintained as previously described (28). Hep G2 (high) cells (*passage 2*) were obtained from ATCC (Rockville, MD). Hep G2 (low) cells (*passage 300*) were kindly provided by Dr. Lucyndia Marino (Cleveland, OH). These cells were designated high or low on the basis of their ability to bind SECR ligands C105Y and C1315 (see below). HuH7 cells were cultured in RPMI medium. Fresh medium was added every second day. All transfection experiments were performed in medium containing 10% fetal calf serum (FCS). Serum had no effect on complex stability.

Determination of cell surface SECR binding. Peptide C105Y was radioiodinated by a modification of the chloramine T method (12) and purified on a Sephadex G_{10} column. Specific radioactivity of ^{125}I-labeled peptide C105Y ranged between 3,500 and 11,700 disintegrations·min^{-1}·ng^{-1}. Binding studies were conducted on HuH7 cells and two populations of Hep G2 cells as previously described (15). Binding parameters were determined by Scatchard analysis. Assays were performed on all three cell lines [HuH7, Hep G2 (high), and Hep G2 (low)] simultaneously with the same batch of iodinated C105Y peptide so that comparison between cell lines could be made.

Production of cDNA complexes that target the SECR. Two features of this system are critical for successful introduction of genes into the cells: *1*) efficient coupling of the DNA-condensing agent, poly-L-lysine, to the peptide used to target the SECR and *2*) proper condensation of the DNA by the peptide-based carrier into highly compact complexes suitable for efficient internalization via an endocytic pathway. Peptides covalently linked to poly-L-lysine (average relative mol mass = 22.5 kDa) with the use of the heterobifunctional crosslinking reagent LC-sulfo-SPDP, as previously described (17). Briefly, 77 μl of 20 mM LC-sulfo-SPDP in water were incubated with 3 mg poly-L-lysine (10-fold molar excess of LC-sulfo-SPDP to polylysine) in 0.1 M phosphate-buffered saline (PBS), pH 7.4, at room temperature (~22°C) for 30 min. The reaction mixture was then dialyzed exhaustively to remove unreacted LC-sulfo-SPDP and low molecular weight reaction products. A threefold molar excess of modified poly-L-lysine was then added to peptide C1315, and the reaction was allowed to proceed at 22°C for 24 h. The conjugate was dialyzed to remove unreacted peptide and low molecular weight reaction products.

Nuclear magnetic resonance spectra. An aliquot (5–10 mg) of the conjugate was exhaustively dialyzed against water, lyophilized from water, and subsequently from D_2O, then resuspended in 0.75 ml of 99.99% D_2O (Aldrich), or 90% dimethyl sulfoxide d6 ($DMSO_{d6}$)-10% D_2O. Proton nuclear magnetic resonance (NMR) spectra were obtained at 600 MHz on a Varian Unity Plus 600 NMR spectrometer using standard proton parameters. Spectra acquisitions typically required between 0.5 and 16 h. Chemical shifts were referenced to the residual water HDO resonance at ~4.8 parts/million (ppm) or the $DMSO_{d6}$ multiplet at 2.5 ppm. Spectra of C1315 peptide and C1315-poly-L-lysine conjugate were obtained in 90% $DMSO_{d6}$. Aliquots of dialysis bath water as well as dialysis bag wash were also lyophilized and examined by NMR to verify the absence of contaminants.

Reporter genes and plasmid preparation. Three plasmids coding for three different reporter genes were used. The expression plasmid pGL3 control (Promega) encodes the *Photinus pyralis* luciferase gene and was inserted into the *Escherichia coli* pUC19 vector. The plasmids pCMV *lac* Z II (20) and pFIX (originally obtained from Dr. Earl Davie, University of Washington, Seattle, WA) contained the cytomegalovirus (CMV) promoter ligated to the *E. coli* β-galactosidase (*lac* Z) and the human factor IX (hFIX) genes, respectively. Plasmids were grown and purified as previously described (21). The sizes of the plasmids were as follows: pGL3, 5.6 kb; pCMV *lac* Z, 10.8 kb; pCMV FIX, 5.4 kb.

Formation of the C1315 peptide-based DNA complexes. The cDNA complexes were formed with the use of general techniques previously described for the galactosylated polylysine ligand (25). The final volume of the solutions was typically 500 μl (0.5–1 μg plasmid DNA/5 μl), containing a mixture of 1:0.45 (wt/wt) DNA-to-peptide-poly-L-lysine conjugate ratio in 0.8–1 M NaCl. Different final concentrations of sodium chloride were due to minor differences among preparations in DNA and poly-L-lysine size and physical state (25). An aliquot of the reaction mixture was examined under the electron microscope (EM) to assess condensation.

Electron microscopy of the condensed DNA complexes. Micrograph grids were prepared as previously described (25). Briefly, immediately after formation of DNA complexes, a drop of a solution (1:10 dilution of complex mixture in water) was added to a 1,000-mesh EM carbon grid, blotted, and stained with 0.04% uranyl acetate. The samples were then shadowed with the use of rotary shadowing and examined using a JEOL-100C EM.

Transfection of hepatoma cells in culture. For pGL3 control, pCMV *lac* Z II, and pFIX transfection, the HuH7 or Hep G2 cells were washed twice with PBS, pH 7.4, trypsinized with 0.05% trypsin in Dulbecco's minimal medium (DMEM), and plated in six-well plates in 10% serum DMEM with glutamine

2 days before transfection. The cells were allowed to adhere to the plate and become 30% confluent. Cell density was typically 5×10^5 cells per plate at the time of transfection. On the day of transfection, growth medium was changed and the cells were washed with Ca^{2+}/Mg^{2+} PBS. Aliquots containing C1315 peptide-poly-L-lysine-DNA complex [0.83, 1.11, or 1.34 pmol pGL3 control, pFIX (0.83 or 1.11 pmol), or pCMV *lac* Z II (0.83, 1.11, or 1.34 pmol) DNA condensed with 62 (122 for *lac* Z II), 80 (160), or 97 (194) pmol C1315-polylysine conjugate, respectively] were added to 2 ml of serum-containing medium in individual wells. Controls included: *1*) HuH7 or Hep G2 (high) (as determined by radioligand binding assay) cells transfected with 1.11 pmol pGL3 control, pFIX, or pCMV *lac* Z II DNA alone, condensed with 80 (160 for *lac* Z II) pmol unconjugated, or condensed with LC-sulfo-SPDP-modified polylysine in the presence of 80 (160) pmol C1315 peptide and 200 (400) pmol LC-sulfo-SPDP linker; *2*) Hep G2 (low) cells transfected with 1.11 pmol pGL3 control or pCMV *lac* Z II DNA condensed with 80 or 160 pmol C1315-polylysine conjugate, respectively; *3*) Hep G2 (high), Hep G2 (low), or HuH7 cells transfected with 1.0 pmol of pGL3 control, pFIX, or pCMV *lac* Z II DNA by lipofectin; *4*) Hep G2 (high), Hep G2 (low), or HuH7 cells transfected with 1.11 pmol of polylysine-condensed DNA by lipofectin. *Controls 1* and *2* were designed to test for nonspecific uptake; *controls 3* and *4* were designed to confirm that target cells could express the transgene if delivered. After addition of the complex and/or lipofectin, all cells were incubated at 37°C for 6 h. Cells were then rinsed with Ca^{2+}/Mg^{2+} PBS, and fresh growth medium was added and incubated at 37°C (with a change of medium every 2 days) until the functional assay was performed. Competition experiments were conducted, transfecting Hep G2 (high) cells with 1.11 pmol C1315 carrier-condensed DNA in the presence and absence of free C1315 peptide (fresh medium was added after 2 h of incubation). All transfections were done in duplicate. No cell death was observed in any of the wells transfected with the DNA-conjugated polylysine complexes throughout the incubation. Luciferase expression was assessed at 2, 4, 6, 8, 10, and 12 days after transfection. Staining for β-galactosidase was done 36 h after transfection. Medium from cells transfected with pFIX was assayed for hFIX 4 days after transfection.

Assay for luciferase expression. Duplicate samples of cells were harvested and assayed for luciferase activity as previously described (3). Protein was determined by the Bradford method (Bio-Rad kit). Results were expressed as integrated light units (ILU) per milligram protein. All measurements were done in duplicate and averaged.

Assay for β-galactosidase activity. Individual HuH7 and Hep G2 cells expressing β-galactosidase were identified as previously described (19). Briefly, cells transfected with the pCMV *lac* Z II plasmid were thoroughly washed with PBS, fixed (in the 6-well plates) with a solution of 0.5% glutaraldehyde in PBS for 10 min, washed again, then incubated in a solution containing 0.5% X-gal for 4–5 h at 37°C. Cells were then lightly counterstained with nuclear fast red. Blue-colored cells were identified and photographed through a phase-contrast inverted-light microscope. Efficiency was calculated by the number of clearly blue cells in 100 cells counted.

Assay for hFIX production. hFIX was assayed by enzyme-linked immunosorbent assay (ELISA). Standards, ranging in concentration from 0.2 to 1 ng/ml, were prepared using purified hFIX (American Diagnostics, Greenwich, CT). ELISA plates were coated with the capturing monoclonal mouse immunoglobulin G (IgG)-derived anti-hFIX (Hematological Technology, Essex, VT), incubated at 4°C overnight, thoroughly rinsed 0.1% Tween 20 PBS, and blocked with 100 μl of 10% FCS in RPMI medium (GIBCO). Standards and aliquots of media collected from transfected HuH7 and Hep G2 cells were then added and incubated at room temperature for 2 h. After stringent wash, 50 μl of primary antibody (rabbit IgG-derived polyclonal anti-hFIX; California Biotechnology) diluted in 10% FCS RPMI (1:1,000) was added to the wells and incubated at room temperature for 1 h. After a stringent wash, 50 μl of a 1:2,000 dilution in 10% FCS RPMI of goat anti-rabbit IgG conjugated to horseradish peroxidase (Boehringer Mannheim) was added. After the final wash, horseradish peroxidase activity in each sample was assessed by optical density measurement of the samples after incubation for 1 h with tetramethyl benzidine dihydrochloride. All assays were done in duplicate, and the results were expressed as nanograms hFIX per milliliter medium per million cells ($ng \cdot ml^{-1} \cdot 10^6\ cells^{-1}$).

β-Galactosidase-SECR cytochemical staining colocalization. HuH7, Hep G2 (high), and Hep G2 (low) cells were plated in six-well plates and transfected as described above. Fluorescein labeling was carried out with fluorescein isothiocyanate, as described previously (22). Two days after transfection, cells were washed with Ca^{2+}/Mg^{2+} PBS, incubated with 100 nM fluorescein-labeled C1315 peptide, and diluted in binding buffer (DMEM containing 50 mM *N*-2-hydroxyethylpiperazine-*N'*-2-ethanesulfonic acid, 0.1 mg/ml cytochrome *c*, 0.01% Tween 80, 2 mg/ml bovine serum albumin) at 4°C. Individual cells were imaged on a Zeiss axiovert 35 microscope at an excitation wavelength of 493.5 nm and a measurement wavelength of 530 nm. Digital images were captured by a cooled CCD camera model CH250 (Photometrics, Tucson, AZ) and quantified by a Nu 2000 camera controller board (Photometrics) with a Macintosh Quadra 900 configuration. Data were processed with Oncor image software (Oncor Imaging, Rockville, MD). After measurement, the cells were rinsed repeatedly and the plates were marked for future reference of orientation. The cells were then assayed for β-galactosidase activity, imaged on a phase-contrast light microscope in the exact orientation used during fluorescein measurements. Photographs were taken to scale to compare cell binding and uptake of fluorescein-labeled C1315 with cellular expression of β-galactosidase.

Statistical analysis. Data are expressed as means ± SE. Statistical comparisons of treatment groups were evaluated with the use of a parametric analysis of variance using the Student-Newman-Keuls test.

RESULTS

Structure of the gene transfer complex. Construction of the protein conjugate of poly-L-lysine to C1315 peptide was monitored by proton NMR, both at the step of LC-sulfo-SPDP modification of polylysine and at the step of conjugation of the C1315 peptide to modified polylysine. Key to the analysis is the presence of unique aromatic proton resonances that have chemical shifts distinct from peaks produced by polylysine for both the LC-sulfo-SPDP conjugated to polylysine and for the C1315 peptide conjugated to SPDP-polylysine. Integration of these resonances relative to the C α-protons of polylysine reveal that 1 in 14 lysine side chains were reacted with the LC-sulfo-SPDP reagent, and 1 in 345–385 lysines were modified by C1315.

Because tightly condensed particles apparently increase the efficiency of internalization, we examined our complexes by electron microscopy. Typically, C1315-polylysine-pGL3 control DNA (5.5 kb) complex mix-

tures contained complexes between 17 and 23 nm in diameter (Fig. 1*C*). Solutions used to make the complexes (high-salt conditions) were also examined and contained no visible structures. The lighter zones bordering the complexes, produced by rotary shadowing, indicate that the height is comparable to the diameter, i.e., the complexes are roughly spherical. Figure 1*A* shows aggregated complexes present in solution before the addition of 5 M NaCl (MATERIALS AND METHODS). Final complex mixtures contained ≤0.5% of these aggregates. Mixtures that contained ≥50% of the aggregated form failed to transfect HuH7, Hep G2 (high), or Hep G2 (low) cells (data not shown). In addition, some complexes appear to unravel at lower salt concentrations into more relaxed crescentlike structures. Mixtures containing these complexes achieved a very low transfection efficiency (data not shown). These data are consistent with previous reports showing that only tightly formed complexes transfect cells efficiently (9). Because plasmid size might affect the size of these particles, the pCMV *lac* Z II DNA (10.8 kb) and C1315-polylysine-pCMV *lac* Z II complexes were compared (Fig. 1*B*). These complexes also ranged in size from 20 to 25 nm in diameter. Complexes with pFIX (5.4 kb) were identical to pGL3 control complexes in size.

Determination of surface receptor binding. HuH7, Hep G2 (high), and Hep G2 (low) cells were incubated with different concentrations of ^{125}I-labeled C105Y peptide in the presence and absence of 200-fold molar excess of unlabeled peptide. Both HuH7 and Hep G2 (high) cells exhibited specific and saturable binding, as shown in Fig. 2. Scatchard analysis of Hep G2 (high) binding revealed a K_d of 48.7 ± 2.4 nM, consistent with previous reports (13, 16, 18, 27, 28). HuH7 cells bound more C105Y [1.5-fold more than Hep G2 (high)] with a K_d of 76.3 ± 7.3 nM. Hep G2 (low) cells exhibited 10-fold less specific binding of iodinated ligand than HuH7 cells and 7.5-fold less than Hep G2 (high) cells (Fig. 2).

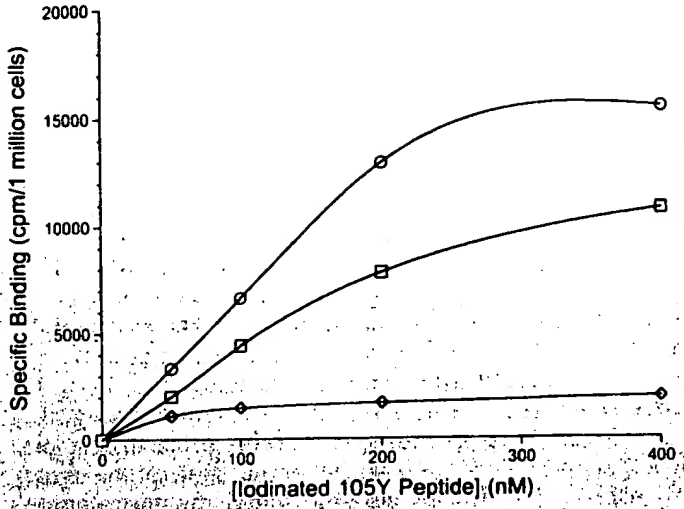

Fig. 2. Specific binding of iodinated C105Y to hepatoma cell lines HuH7 (○), Hep G2 (high) (□), and Hep G2 (low) cells (◇). Specific binding represents difference between total binding and binding in the presence of 200-fold excess of unlabeled peptide (nonspecific binding). A representative example from 6 experiments is shown. cpm, Counts/min.

Hep G2 (low) cells bound iodinated C105Y with a K_d of 124.2 ± 34.2 nM. These binding trends were consistent in seven experiments that compared binding in HuH7, Hep G2 (high), and Hep G2 (low) cells.

Transfection of Hep G2 cells with the pGL3 control luciferase expression plasmid. Various concentrations of C1315-polylysine-pGL3 control DNA complexes were applied to Hep G2 cells. Transfection and expression were assessed by luciferase enzyme activity in cell extracts. Positive controls, described in MATERIALS AND METHODS, established the capability of both Hep G2 (high) and Hep G2 (low) cells to express the pGL3 luciferase gene product. Luciferase activity transfected by receptor-mediated means peaked at 538,731 ±

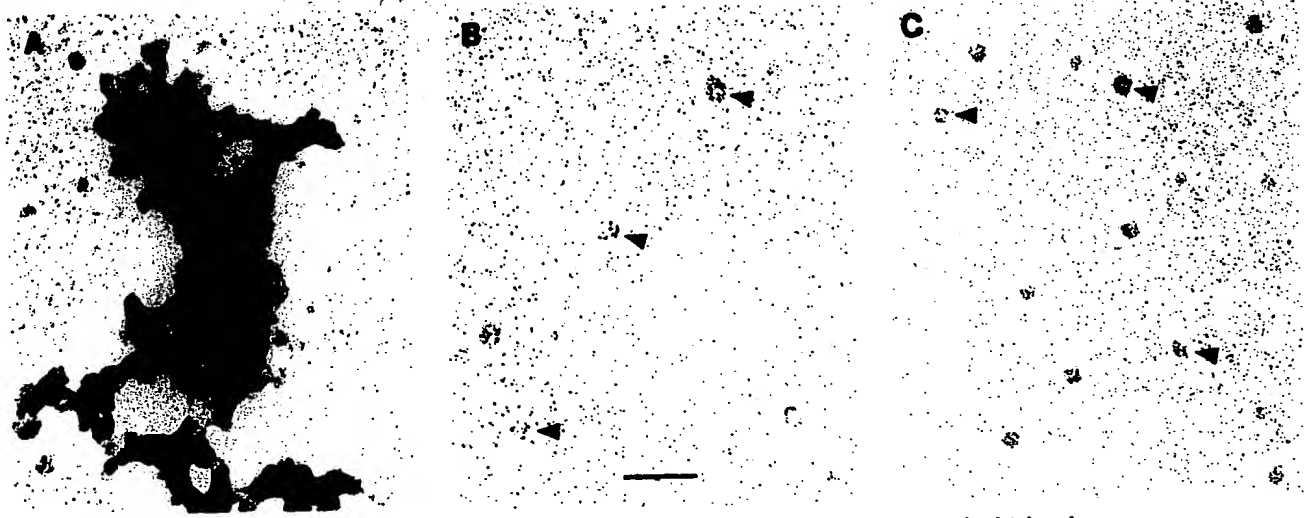

Fig. 1. Electron micrographs of C1315-polylysine condensed plasmid DNA. Complexes were formed under high-salt conditions (~1 M), then diluted 10 times and immediately pipetted onto a 1,000-mesh electron microscope carbon grid, fixed, blotted, and stained with 0.04% uranyl acetate. *A*: aggregated complexes [formed under low-salt (~ 0.3 M) conditions]. *B*: spheroid particles observed when cytomegalovirus (CMV) *lac* Z II plasmid [10.8 kilobase (kb)] was properly condensed (arrowheads). *C*: spheroid particles observed when SV40 pGL3 control plasmid (5.25 kb) was properly condensed (arrowheads). Bar, 100 nm.

144,346 ILU/mg protein between *days 2* and *4*. Luciferase activity declined to background 10 days after transfection. Figure 3*A* demonstrates the dose dependence and time course of the transfection with the peptide-based complex. Gene transfer was greatest with DNA content of 1.11 pmol/5 × 10^5 cells in a 10-mm well. Complex concentrations either below or above the optimum concentration achieved less efficient transfer and expression (8, 25, 32). Hep G2 (low) cells were transfected by the complex with a much lower efficiency (Fig. 3*A*).

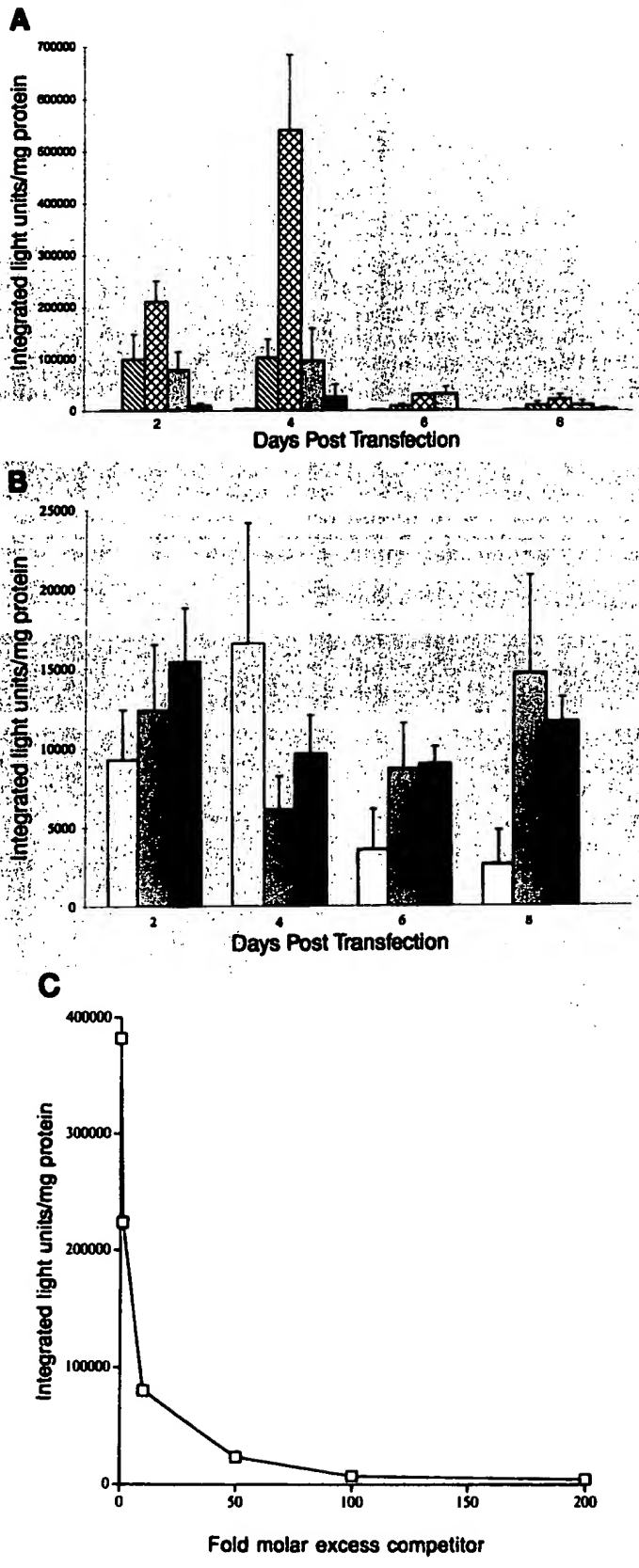

Fig. 3. Luciferase expression: dose dependence and time course of expression. *A*: luciferase activity assayed 2, 4, 6, and 8 days after transfection with 0.83 pmol (hatched bars), 1.11 pmol (crosshatched bars), or 1.34 pmol (shaded bars) of pGL3 plasmid DNA. Protein extracts obtained from cells treated with 1.34 pmol of pGL3 plasmid DNA condensed with unmodified poly-L-lysine in the presence of free peptide were used as negative controls (open bars). In the 6 experiments performed, all DNA concentrations produced significant ($P < 0.05$) transgene expression at *days 2* and *4*. Hep G2 (high) expression was statistically significant from Hep G2 (low) (black bars) expression at *days 2*, *4*, and *6*. None of the transfected Hep G2 (low) samples were significantly different from negative controls. Lipofectin transfection yielded similar transfection in both cell types: Hep G2 (high), 1,023,000; and Hep G2 (low), 934,000 integrated light units (ILU)/mg protein. *B*: luciferase expression in cells transfected with nonfunctional conjugates. In the 6 experiments conducted, 1.11 pmol of DNA properly condensed with either poly-L-lysine (open bars) or poly-L-lysine modified with LC-sulfo-*N*-succinimidyl-3-(2-pyridyldithio)propionate (SPDP; gray bars) in the presence of free C1315 peptide failed to result in luciferase activity significantly different from cells incubated with naked DNA (black bars). All controls were significantly less effective than active complex. Note different scale on *y*-axis. *C*: dose-dependent competition of transgene expression with free ligand. Hep G2 (high) cells were transfected with optimal DNA concentration (1.11 pmol) in the presence and absence of a 1-, 10-, 50-, 100-, and 200-fold molar excess of free C1315 peptide. Fold molar excess competitor refers to free C1315 added in excess to peptide conjugated to the transfection complexes. Inhibited expression levels differed from uninhibited transfection ($P < 0.05$).

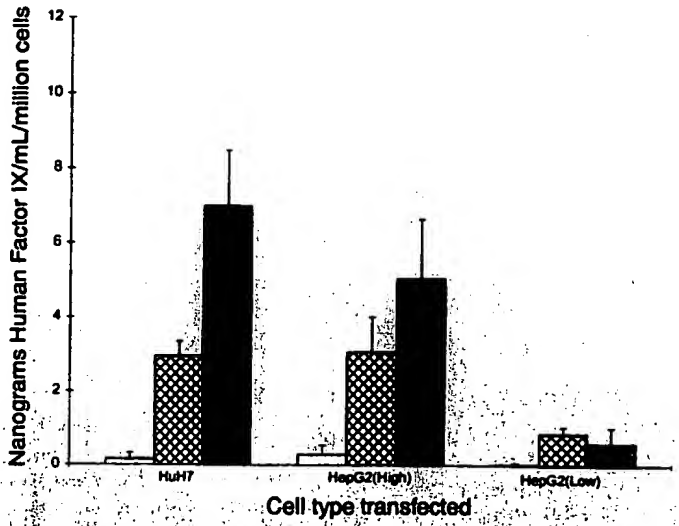

Fig. 4. Human factor IX expression in transfected cells. HuH7, Hep G2 (high), and Hep G2 (low) cells were transfected with control complexes (open bars), 0.83 pmol (crosshatched bars), and 1.11 pmol of CMV pFIX plasmid coding for human coagulation factor IX (black bars). Human factor IX secreted into the media was assayed at 4 days posttransfection by enzyme-linked immunosorbent assay for human factor IX. In the 5 experiments performed, HuH7 and Hep G2 (high) cells expressed levels of human factor IX that were significantly higher ($P < 0.05$) than Hep G2 (low). HuH7 and Hep G2 (high) cell expression was also significantly different from control transfections ($P < 0.05$), whereas Hep G2 (low) cell expression was not. Lipofectin transfection yielded similar results in all 3 cell types: HuH7, 22.35; Hep G2 (high), 25.45; and Hep G2 (low) 26.74 ng·ml^{-1}·million $cells^{-1}$.

Table 1. *Transgene and SECR expression in hepatocytes*

Cell Type	Average %Blue Cells	Average %Fluorescent Cells
Hep G2 (high)	11.3 ± 2.3	20.4 ± 4.6
HuH7	5.0 ± 1.5	14.3 ± 1.6
Hep G2 (low)	1.0 ± 0.4	1.8 ± 0.6

Data are means ± SE; $n = 6$ experiments for each cell type. HuH7, Hep G2 (high), and Hep G2 (low) cells were treated with 1.11 pmol of CMV *lac* Z II plasmid DNA condensed with peptide carrier. Cells were assayed for β-galactosidase activity 3 days after transfection. Percentages represent number of clearly blue or fluorescent cells per 100 cells counted. SECR, serpin enzyme complex receptor.

Hep G2 (high) cells exposed to unconjugated poly-L-lysine-condensed DNA (1.11 pmol), as well as LC-sulfo-SPDP modified poly-L-lysine-condensed DNA (1.11 pmol) in the presence of corresponding concentrations of free C1315, were not transfected (Fig. 3*B*).

Addition of a 1-, 10-, 50-, 100-, and 200-fold molar excess of free peptide at the time of transfection blocked uptake and expression in a dose-dependent fashion, as shown in Fig. 3*C*. High excess of peptide completely blocked uptake and transfection. Excess free peptide had no effect on cell viability.

Transfer of hFIX to Hep G2 cells. We tested the ability of our system to deliver a clinically relevant gene as well. Hep G2 and HuH7 cells do not express endogenous human coagulation factor IX. Thus we transduced cells with a plasmid coding for the hFIX gene and measured product secreted into growth medium 4 days later. The medium did not interfere with ELISA for factor IX. Figure 4 depicts the results. When transfected with 1.11 pmol carrier-condensed DNA, HuH7 cells produced 7.01 ± 1.49 ng/ml, whereas Hep G2 (high) cells produced 5.07 ± 1.60 ng/ml hFIX. As with other reporter genes, Hep G2 (low) cells expressed minimal factor IX, peaking at 0.86 ± 0.44 ng/ml, with 1.11 pmol carrier-condensed DNA. Again, unconjugated poly-L-lysine-condensed DNA failed to transduce any of the cell types.

Transfection with pCMV lac Z II β-galactosidase expression plasmid. Both HuH7 and Hep G2 cell lines were transfected with the pCMV *lac* Z II plasmid coding for the β-galactosidase protein as described above. As shown in Table 1, HuH7 and Hep G2 (high) cells, but not Hep G2 (low), displayed substantial β-galactosidase staining. The pattern of staining varied with DNA concentration, similar to luciferase expression. For both HuH7 and Hep G2 (high), 1.11 pmol DNA/well produced the highest percentage of positive cells (Table 1). Nonspecific lipofectin transfection of cells yielded, on average, twice the proportion of positive cells seen with our complex. DNA condensed with unconjugated C1315-poly-L-lysine failed to transfect any of the cell types. Positive cells were intensely stained, and no background β-galactosidase activity was detected.

Colocalization of SECR and β-galactosidase expression. We designed a set of experiments to colocalize transgene expression with expression of SECR. Cytochemical staining for the receptor with fluorescein-labeled C1315 peptide revealed that only some cells in cultures of HuH7, Hep G2 (high), and Hep G2 (low) cells bind detectable amounts of the ligand (shown in Table 1). Only those Hep G2 (high) and HuH7 cells that bound the fluorescein-labeled peptide took up the complex, expressed the transgene, and stained positive for β-galactosidase expression. Hep G2 (low) cells exhibit-

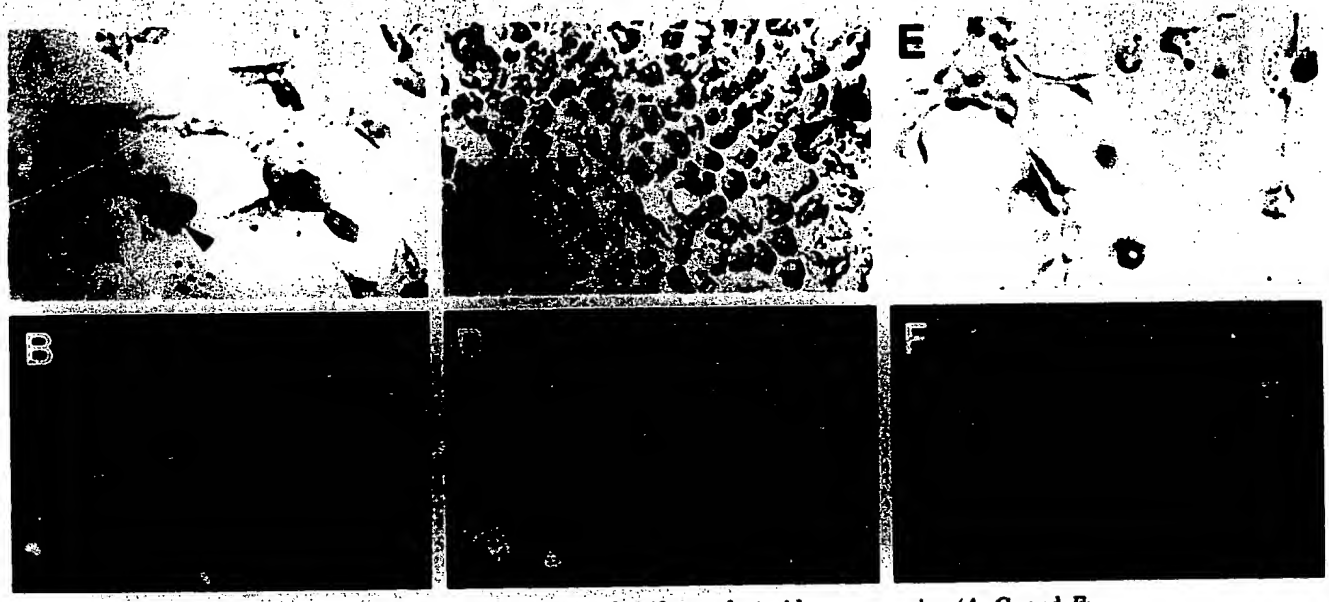

Fig. 5. Comparison of cellular or histochemical staining to identify β-galactosidase expression (*A*, *C*, and *E*; arrowheads indicate blue-stained cells) and immunofluorescent identification of cells that express high levels of serpin enzyme complex receptor (SECR; *B*, *D*, and *F*). *A* and *B*: HuH7 cells. *C* and *D*: Hep G2 (high) cells. *E* and *F*: Hep G2 (low) cells. Same field was photographed for each pair. No example was found of a cell positive for β-galactosidase expression that was not also positive for SECR expression, but not all SECR-positive cells stained intensely for β-galactosidase activity. Lipofectin transfection of Hep G2 (high) cells yielded 34.8 ± 6.7; HuH7 cells, 14.7 ± 3.6; and Hep G2 (low), 9.7 ± 1.6 blue cells in 100 cells counted. Magnification ×20.

ing minimal fluorescence did not stain positive for β-galactosidase. Furthermore, HuH7 cells bound the fluorescein-labeled peptide with less frequency than Hep G2 (high) cells (Table 1). However, HuH7 binding, as well as β-galactosidase expression, was more intense (Fig. 5, *A* and *B*, respectively). Cells treated with unlabeled peptide or free fluorescein had no detectable autofluorescence.

DISCUSSION

We have shown that expression plasmids tightly condensed (18–25 nm in diameter) with polylysine conjugated to the C1315 peptide, a ligand previously shown to bind to the SECR (13, 16, 26–28), can be targeted to cells bearing the receptor in vitro. The size of the peptide ligand, as well as the repetitive nature of poly-L-lysine, allows us to assess the coupling of the C1315 peptide to the poly-L-lysine by NMR, which demonstrates that one receptor ligand for every three poly-L-lysine molecules (or 35 and 72 ligands bound to each of the small and large plasmid DNA molecules, respectively) is sufficient to direct receptor-mediated gene transfer. At the structural level, we are able, using electron microscopy, to verify that compact condensation occurs. Our data confirm that tightly condensed complexes are far more efficient for transfection than the aggregates that form at lower NaCl concentrations or relaxed complexes that form at higher NaCl concentrations.

Several lines of evidence indicate that gene transfer is mediated by the SECR and does not occur by nonspecific mechanisms. Hep G2 (low) cells, which express few SECRs, take up and express minimal levels of DNA (although they are capable of expressing the identical plasmid when it is delivered by lipofectin), whereas HuH7 and Hep G2 (high) cells, which express abundant SECR, can be transduced with a 10-fold higher efficiency. This is true for all genes tested. In addition, free ligand added at the time of transfection inhibited gene transfer in a dose-dependent manner, so receptor ligands apparently compete with the complex for receptor binding and uptake. HuH7 and Hep G2 (high) cells transfected with DNA condensed with unmodified polylysine in the presence or absence of free peptide did not exhibit gene expression, so uptake is not due to nonspecific pinocytosis of condensed DNA particles. Only cells shown by fluorescent ligand binding and uptake to bind the C1315 peptide exhibit intense β-galactosidase activity, whereas cells that bind no fluorescent C1315 do not express the *lac* Z gene. Taken together, these data demonstrate that uptake and expression of exogenous genes are mediated through the SECR.

The specificity, as well as success, of gene transfer in vitro in cells that bear the SEC receptor allows us to speculate that this receptor system could promote gene transfer in vivo. High-level expression was achieved for all three reporter genes. In addition, substantial gene transfer occurred even in the presence of a 10-fold molar excess of competitive ligand in vitro, so the presence of the natural ligand in vivo will probably not prohibit gene transfer. SECR has been found in lung, liver, and brain (reviewed in Ref. 26), all of which might be potential target tissues for therapeutic gene transfer in common inherited (e.g., α_1-AT deficiency) or acquired (e.g., Alzheimer's disease) disorders.

Thus the tissue distribution of the SECR coupled to the specificity and in vitro success of SECR-directed gene transfer give this system promise for gene therapy. However, more detailed knowledge of receptor-mediated gene transfer and the elements that affect its efficiency is crucial to optimizing the system for gene therapy. The SECR-directed system offers special advantages in this regard, because NMR can be used to assess the stoichiometry and internal structure of the protein portion of the gene transfer complex and the receptor ligand can be labeled with fluorescent tags for tracking its fate inside the cell. In addition, examination of the in vivo response to targeting this system (for example, immune responses or receptor-mediated signal transduction) is essential to evaluate the potential of this system for therapeutic use.

The authors thank Dianne Kube and Andrew Martin for assistance with photomicrography. In addition, we thank Lloyd Culp (Case Western Reserve University, Cleveland, OH) for providing the pCMV *lac* Z II plasmid and Catherine L. Silski for technical support.

This study was supported by National Institutes of Health Grants DK-49138, DK-43999, and P30-DK-27651 to P. Davis, T32-HL-07653 to A. Ziady, HL-37784 and AG-11577 to D. Perlmutter, and the Burroughs Wellcome Fund to D. Perlmutter.

Address for reprint requests: P. B. Davis, Dept. of Pediatrics, Case Western Reserve Univ., 11100 Euclid Ave., Cleveland, OH 44106.

Received 25 October 1996; accepted in final form 1 May 1997.

REFERENCES

1. **Banda, M. J., A. G. Rice, G. L. Griffin, and R. M. Senior.** The inhibitory complex of human alpha-1-proteinase inhibitor and human leukocyte elastase is a neutrophil chemoattractant. *J. Exp. Med.* 167: 1608–1615, 1988.
2. **Boland, K., K. Manias, and D. H. Perlmutter.** Specificity in recognition of amyloid-β peptide by the serpin enzyme complex receptor in hepatoma cells and neuronal cells. *J. Biol. Chem.* 270: 28022–28028, 1995.
3. **Brasier, A. R., J. E. Tate, and J. F. Habener.** Optimized use of firefly luciferase assay as a reporter in mammalian cell lines. *Biotechniques* 7: 1116–1122, 1989.
4. **Bu, G., P. A. Morton, and A. L. Schwartz.** Identification and partial characterization by chemical cross-linking of a binding protein for tissue-type plasminogen activator (t-PA) on rat hepatoma cells. *J. Biol. Chem.* 267: 15595–15602, 1992.
5. **Collins, F. S.** Cystic fibrosis: molecular biology and therapeutic implications. *Science* 256: 774–779, 1991.
6. **Cotten, M., E. Wagner, K. Zatloukal, S. Phillips, D. T. Curiel, and M. L. Birnstiel.** High-efficiency receptor-mediated delivery of small and large (48 kilobase) gene constructs using endosome-disruption activity of defective or chemically inactivated adenovirus particles. *Proc. Natl. Acad. Sci. USA* 89: 6094–6098, 1992.
7. **Drumm, M. L., H. A. Pope, W. H. Cliff, J. M. Rommens, S. A. Marvin, L. C. Tsui, F. S. Collins, R. A. Frizzell, and J. M. Wilson.** Correction of the cystic fibrosis defect in vitro by retrovirus-mediated gene transfer. *Cell* 62: 1227–1233, 1990.
8. **Ferkol, T., C. S. Kaetzel, and P. B. Davis.** Gene transfer into respiratory epithelial cells by targeting the polymeric immunoglobulin receptor. *J. Clin. Invest.* 92: 2394–2400, 1992.
9. **Ferkol, T., J. C. Perales, F. Mularo, and R. W. Hanson.** Receptor-mediated gene transfer into macrophages. *Proc. Natl. Acad. Sci. USA* 93: 101–105, 1996.

10. **Flotte, T., S. Afione, R. Solow, and P. I. Carter.** Expression of CFTR from AAV vectors (Abstract). *Pediatr. Pulmonol.* 8, *Suppl.*: 237, 1992.
11. **Flotte, T. R., R. Solow, R. A. Owens, S. Afione, P. I. Zeitlin, and B. J. Carter.** Gene expression from adeno associated virus vectors in airway epithelial cells. *Am. J. Respir. Cell Mol. Biol.* 7: 349–356, 1991.
12. **Hunter, W. M., and F. C. Greenwood.** Protein determination by a novel radio-iodination method. *Nature* 194: 495–496, 1962.
13. **Joslin, G., R. Fallon, J. Bullock, S. P. Adams, and D. H. Perlmutter.** The SEC-receptor recognizes a pentapeptide neodomain of α_1AT-protease complexes. *J. Biol. Chem.* 266: 11282–11288, 1991.
14. **Joslin, G., G. L. Griffin, A. M. August, S. Adams, R. J. Fallon, R. M. Senior, and D. H. Perlmutter.** The serpin-enzyme complex (SEC) receptor mediates the neutrophil chemotactic effect of α_1-antitrypsin-elastase complexes and amyloid-β peptide. *J. Clin. Invest.* 90: 1150–1154, 1992.
15. **Joslin, G., J. Krause, A. D. Hershey, S. P. Adams, R. J. Fallon, and D. H. Perlmutter.** Amyloid-β peptide, substance P, and bombesin bind to the serpin enzyme complex receptor. *J. Biol. Chem.* 266: 21897–21902, 1991.
16. **Joslin, G., A. Wittwer, S. Adams, D. M. Tollefsen, A. August, and D. H. Perlmutter.** Cross competition for binding of α_1AT-elastase complexes in the serpin enzyme complex receptor by other serpin enzyme complexes and by proteolytically modified α_1-AT. *J. Biol. Chem.* 268: 1886–1893, 1993.
17. **Jung, G., W. Kohnlein, and G. Luders.** Biological activity of the antitumor protein neocarzino statin coupled to a monoclonal antibody by *N*-succinimidyl-3(2-pyridyldithio) propionate. *Biochem. Biophys. Res. Commun.* 101: 599–606, 1981.
18. **Kahalil, Z., K. Sanderson, P. Isberg, M. Bassirat, B. Livett, and R. Helme.** βA_4 25–35 modulates substance P effects on rat skin microvasculature in aged rats: pharmacological manipulation using SEC-receptor ligands. *Brain Res.* 651: 227–235, 1994.
19. **Lim, K., and C. B. Chase.** A simple assay for DNA transfection by incubation of the cells in culture dishes with substrates for beta-galactosidase. *Biotechniques* 7: 576–579, 1989.
20. **Lin, W. C., and L. A. Culp.** Selectable plasmid vectors with alternative and ultrasensitive histochemical marker genes. *Biotechniques* 11: 344–351, 1991.
21. **Maniatis, T., E. F. Fritsch, and J. Stambrook.** *Molecular Cloning: A Laboratory Manual.* Cold Spring Harbor, NY: Cold Spring Harbor Laboratory Press, 1989.
22. **Mann, K. G., and W. Fish.** Protein polypeptide chain molecular weights by gel chromatography in guanidinium chloride. *Methods Enzymol.* 26: 28–42, 1972.
23. **Michael, S. I., and D. T. Curiel.** Strategies to achieve targeted gene delivery via the receptor mediated endocytosis pathway. *Gene Ther.* 1: 223–232, 1994.
24. **Miller, D. G., M. A. Adam, and A. D. Miller.** Gene transfer by retrovirus vectors occurs only in cells that are actively replicating at the time of infection. *Mol. Cell. Biol.* 10: 4239–4242, 1991.
25. **Perales, J. C., T. Ferkol, H. Beegen, O. D. Ratnoff, and R. W. Hanson.** Gene transfer in vivo: sustained expression and regulation of genes introduced into the livers by receptor targeted uptake. *Proc. Natl. Acad. Sci. USA* 91: 4086–4090, 1994.
26. **Perlmutter, D. H.** The SEC receptor: a possible link between neonatal hepatitis in α_1AT deficiency and Alzheimer's disease. *Pediatr. Res.* 36: 271–277, 1994.
27. **Perlmutter, D. H., G. L. Glover, M. Meheryar, C. S. Schasteen, and R. J. Fallon.** Identification of a serpin-enzyme complex (SEC) receptor on human hepatoma cells and human monocytes. *Proc. Natl. Acad. Sci. USA* 87: 3753–3757, 1990.
28. **Perlmutter, D. H., G. Joslin, P. Nelson, C. S. Schasteen, S. P. Adams, and R. J. Fallon.** Endocytosis and degradation of α-1-antiprotease protenase complexes are mediated by the SEC receptor. *J. Biol. Chem.* 265: 16713–16716, 1990.
29. **Rosenfeld, M. A., K. Yoshimura, B. C. Trapnell, K. Yoneyama, E. R. Rosenthal, W. Dalemans, M. Fukayama, J. Bargon, L. E. Stier, and L. Stratford-Perricaudet.** Expression of the cystic fibrosis transmembrane conductance regulator gene to the airway epithelium. *Cell* 68: 143–155, 1992.
30. **Wagner, E., M. Cotten, R. Foisner, and M. L. Birnstiel.** Transferrin polycation DNA complexes: the effect of polycations on the structure of the complex and DNA delivery to cells. *Proc. Natl. Acad. Sci. USA* 88: 4255–4259, 1991.
31. **Wagner, E., M. Zenke, M. Cotten, H. Beug, and M. L. Brinstell.** Transferrin polycation conjugates as carriers for DNA uptake into cells. *Proc. Natl. Acad. Sci. USA* 87: 3410–3414, 1990.
32. **Wu, G. Y., and C. H. Wu.** Receptor-mediated in vitro gene transformation soluble DNA carrier system. *J. Biol. Chem.* 262: 4429–4432, 1987.